UC San Diego

UC San Diego Electronic Theses and Dissertations

Title

Predicting Verbal Memory Impairment using Structural Connectomics in Drug-resistant Temporal Lobe Epilepsy

Permalink

https://escholarship.org/uc/item/4nc475c2

Author

Balachandra, Akshara Rao

Publication Date

2019

Peer reviewed|Thesis/dissertation

eScholarship.org Powered by the California Digital Library
University of California

UNIVERSITY OF CALIFORNIA SAN DIEGO

Predicting Verbal Memory Impairment using Structural Connectomics in Drug-resistant Temporal Lobe Epilepsy

A thesis submitted in partial satisfaction of the requirements for the degree
Master of Science

in

Biology

by

Akshara Rao Balachandra

Committee in charge:

Professor Carrie McDonald, Chair
Professor Jill Leutgeb, Co-Chair
Professor Yunde Zhao

2019

Copyright
Akshara Rao Balachandra, 2019
All rights reserved.

The thesis of Akshara Rao Balachandra is approved, and it is acceptable in quality and form for publication on microfilm and electronically:

_____

_____
Co-Chair

_____
Chair

University of California San Diego

2019

DEDICATION

To my Guru Shri Raghavendra Teertharu and to my family, for their love and support

TABLE OF CONTENTS

Signature Page . . . iii

Dedication . . . iv

Table of Contents . . . v

List of Figures . . . vii

List of Tables . . . viii

Acknowledgements . . . ix

Vita . . . x

Abstract of the Thesis . . . xi

1 INTRODUCTION . . . 1
- 1.1 Epilepsy . . . 1
  - 1.1.1 Memory deficits in TLE . . . 1
  - 1.1.2 Histopathological Changes in TLE . . . 3
- 1.2 Alternative neuroimaging analysis methods . . . 3
- 1.3 Diffusion Tensor Imaging . . . 4
  - 1.3.1 Diffusion Tensor Imaging in TLE . . . 5
- 1.4 Connectomes . . . 7
- 1.5 Current study . . . 8

2 METHODS . . . 10
- 2.1 Subjects . . . 10
- 2.2 Neuropsychological testing . . . 11
- 2.3 MRI acquisition . . . 11
- 2.4 DTI processing . . . 12
- 2.5 Fiber tract calculations . . . 12
- 2.6 Volumetrics . . . 13
- 2.7 Structural connectome generation . . . 13
- 2.8 Classification Model . . . 15
- 2.9 Memory Impairment Prediction Model with Connectomes . . . 16
- 2.10 Classification model employing other features . . . 18
- 2.11 Randomization testing . . . 18
- 2.12 Linking principal components from PCA to biological underpinnings . . . 19

3 RESULTS 20
3.1 Patient Demographics and Clinical Variables 20
3.2 Unimodal feature performance 21
3.3 Multimodal feature performance 22
3.4 Important features from each model 22
3.5 Cortical connections contributing the most important PCs 23

4 DISCUSSION 25
4.1 White matter integrity is more important than HCV and clinical features for verbal memory 25
4.2 Connectome adds novel information to tract-based and volumetric analyses 27
4.3 Strengths, limitations, and future directions 29
4.4 Conclusion 31

REFERENCES 46

LIST OF FIGURES

Figure 1: Deep white matter tracts of interest 33
Figure 2: Connectome model pipeline 34
Figure 3: Sample classification model illustrating basic performance measures of machine learning models. 35
Figure 4: Unimodal features receiver operating characteristic (ROC) curves. . . 36
Figure 5: Multimodal features receiver operating characteristic (ROC) curves. . 37
Figure 6: Feature importance plots for each set of unimodal features. 38
Figure 7: Feature importance plots for multimodal prediction models. 39
Figure 8: Connections with highest weight towards principal components. . . . 40
Figure 9: Top 15 most important connections for memory impairment classification. 41

LIST OF TABLES

Table 1: Demographics and clinical variables. 42
Table 2: XGBoost model performance with each set of features. 43
Table 3: Distribution of metrics with randomization testing for each machine learning model. 44
Table 4: Important cortical connections for memory impairment classification . 45

ACKNOWLEDGEMENTS

I first want to thank Dr. Carrie McDonald for making this research possible. Since entering her lab as an undergraduate student, she has helped me grow intellectually and professionally. Carrie has always taken the time to provide guidance in my research and clinical endeavors in the healthcare field. I will forever remember her kindness and mentorship.

I also want to express my gratitude to post-docs Erik Kaestner and Naeim Bahrami for helping me tremendously with formulating the methods and data analysis. Further, I am grateful to Sanam Lalani and Anny Reyes for helping with the neuropsychological data and classification. I want to thank research associate Anna-Christina Macari for running all the MRI pre-processing and providing the imaging data I used in this project. I also want to thank Dr. Leonardo Bonilha for providing an open-source implementation of generating connectomes and helping to analyze the final results of this study.

Finally, I am grateful for Dr. Jill Leutgeb and Dr. Yunde Zhao for being members of my committee.

This thesis, in full, is currently being prepared for submission for publication of the material. Balachandra, Akshara R.; Kaestner, Erik; Bahrami, Naeim; Reyes, Anny; Macari, Anna-Christina; McDonald, Carrie R. The thesis author was the primary investigator and author of this material.

VITA

2018	B. S. in Biochemistry & Cell Biology *summa cum laude*, University of California San Diego
2019	M. S. in Biology, University of California San Diego

PUBLICATIONS

Reyes A, Kaestner E, Bahrami N, **Balachandra A**, Hegde M, Paul BM, Hermann B, McDonald CR. Cognitive phenotypes in temporal lobe epilepsy are associated with distinct patterns of white matter network abnormalities. *Neurology*. 2019 Mar 27:10-212.

Reyes A, Uttarwar VS, Chang YH, **Balachandra AR**, Pung CJ, Hagler Jr DJ, Paul BM, McDonald CR. Decreased neurite density within frontostriatal networks is associated with executive dysfunction in temporal lobe epilepsy. *Epilepsy & Behavior*. 2018 Jan 1;78:187-93.

Reas ET, Hagler DJ, White NS, Kuperman JM, Bartsch H, Cross K, Loi RQ, **Balachandra AR**, Meloy MJ, Wierenga CE, Galasko D. Sensitivity of restriction spectrum imaging to memory and neuropathology in Alzheimer's disease. *Alzheimer's research & therapy*. 2017 Dec;9(1):55.

Loi RQ, Leyden KM, **Balachandra A**, Uttarwar V, Hagler Jr DJ, Paul BM, Dale AM, White NS, McDonald CR. Restriction spectrum imaging reveals decreased neurite density in patients with temporal lobe epilepsy. *Epilepsia*. 2016 Nov;57(11):1897-906.

ABSTRACT OF THE THESIS

Predicting Verbal Memory Impairment using Structural Connectomics in Drug-resistant Temporal Lobe Epilepsy

by

Akshara Rao Balachandra

Master of Science in Biology

University of California San Diego, 2019

Professor Carrie McDonald, Chair
Professor Jill Leutgeb, Co-Chair

Objective: We aimed to determine whether a novel, white matter (WM) network-based approach (i.e. structural connectomes; SC) outperforms traditional tract-based measures and hippocampal volume (HCV) for discriminating temporal lobe epilepsy (TLE) patients with memory-impairment from those with normal memory.

Methods: T1-and diffusion-weighted imaging (DWI), clinical, and neuropsychological data were available for 81 patients with TLE and 61 healthy controls. Five medial temporal lobe WM tracts were extracted from the DWI and fractional anisotropy (FA) was

calculated for each tract. Left and right HCVs were derived using FreeSurfer. SCs were derived by performing probabilistic tractography and measuring the number of connections among cortical regions. SCs were fed into XGBoost, a robust tree-based classifier. The model was trained on 48 patients from UCSD and tested on 33 patients from UCSF.

Results: Both SCs (76% accuracy) and tracts (73% accuracy) were better classifiers of verbal memory performance than HCV (66% accuracy) or clinical variables (61% accuracy). Within the WM-based models, the SC performed similar to or better than the tract-based models, with slightly higher accuracy and positive predictive value (PPV; 0.81 for SC, 0.77 for tracts). The SC appeared to provide more specific information regarding abnormal connectivity contributing to verbal memory performance. Multivariate models seemed to be most robust classifiers, providing the highest sensitivity (0.95 for Tract+HCV) and specificity (0.67 for Connectome+HCV).

Conclusion: SCs and tract-based measures appear to outperform HCVs and clinical variables for predicting memory impairment in TLE. However, network-based models combined with HCVs may provide the best prediction accuracy.

1 INTRODUCTION

1.1 Epilepsy

Epilepsy is a neurological disorder characterized by recurrent seizures due to excessive rhythmic and synchronous neuronal activity. It is one of the most common neurological conditions, with an estimated 65 million people suffering from epilepsy worldwide (Ngugi et al., 2010). Approximately 30% of those affected are resistant to anti-epileptic drugs (AEDs) (Kalilani et al., 2018). Temporal lobe epilepsy (TLE) is a type of focal epilepsy in which seizures are electrographically localized to the temporal lobe, most often arising from the hippocampus and other medial temporal lobe (MTL) structures (Gastaut et al., 1975). TLE is the most common type of focal epilepsy and has high rates of AED resistance (Engel, 2003). The prevention of recurrent seizures is critical for reducing the risk of sudden death, as well as cognitive and psychiatric comorbidities of epilepsy such as memory and language impairments (Téllez-Zenteno et al., 2005).

1.1.1 Memory deficits in TLE

The most common and often problematic cognitive comorbidity in patients with TLE is memory impairment. Almost half of patients with TLE suffer from some degree of memory impairment (Fisher et al., 2000; Hermann and Seidenberg, 2008), including

problems with both episodic and semantic memory (Saling, 2009). Episodic memory, defined as memory for discrete episodes or events, is particularly impaired in TLE and manifests on neuropsychological tests as problems with list learning and recall, memory for contextual information (i.e., prose memory), and associative learning/recall. However, surgery can pose an additional risk for episodic memory decline if patients are operated on in the "dominant" hemisphere (i.e., the hemisphere the is dominant for language and verbal memory) (Helmstaedter et al., 2003). One of the first conceptualizations of memory impairment in TLE was the material-specificity hypothesis, which posited that the left and right temporal lobes process different types of information and memory, namely verbal and non-verbal respectively (Milner, 1970). However, it is now appreciated that most episodic memories involve both MTLs, and that patients with both right and left TLE can be impaired on a variety of verbal and/or visuospatial episodic memory tasks (Saling, 2009). Despite the broad episodic memory impairments seen in many patients, up to 50% of patients with TLE have normal memory functioning, which may imply normal structural and functional integrity of the MTL.

The risk for post-operative decline in memory is a major factor taken into account in pre-surgical decision making. Patients and their doctors weigh the benefits of seizure freedom with the risk of post-operative memory decline to decide if surgery is the best treatment option. Patients with late onset seizures with no apparent MTL pathology and normal presurgical verbal memory performance are at especially high risk for decline after having left anterior temporal lobectomy (ATL). ATL involves the removal of most of the anterior temporal lobe including the anterior portion of the hippocampus, uncus, amygdala, entorhinal cortex, and temporal lobe white matter. This change in memory-based function is generally attributed to the resection of relatively normal neocortex and the subadjacent white matter in the temporal lobe (Saling, 2009). However, patients who present with MTL

pathology and impaired pre-operative verbal memory performance are at lowest risk for decline post-ATL, as the ATL would likely resect diseased neocortex and white matter, having minimal impact on temporal lobe memory functions (Saling, 2009).

1.1.2 Histopathological Changes in TLE

Mesial temporal lobe sclerosis (MTS) is the most common histopathological abnormality in TLE. MTS is typically identified ipsilateral to the side of seizure onset and is characterized by neuronal cell loss and gliosis that is most prominent in the hippocampus (Wieser, 2004). It is unknown as to whether MTS is the cause or result of seizures in pathologically abnormal patients (Wong and Guo, 2013). However, identification of MTS greatly improves the probability of seizure freedom post-surgery (Engel, 2003). Structural magnetic resonance imaging (MRI) is used clinically to visually identify lesions like MTS, primarily by identifying hippocampal atrophy and loss of internal hippocampal architecture on T1-weighted imaging and T2-weighted imaging. Hippocampal volume (HCV) loss is the most common finding in MTS and there is strong evidence that the degree of HCV loss correlates with the degree of memory impairment (McDonald, 2008). HCV can be easily quantified from standard T1-weighted scans and, for this reason, early studies focused exclusively on the contribution of HCV loss to memory impairment in TLE (Kilpatrick et al., 1997; Griffith et al., 2003, 2004). It soon became clear, though, that these structural abnormalities are not just localized to the hippocampus and other MTL structures, but rather extend throughout the whole brain.

1.2 Alternative neuroimaging analysis methods

In the 1990s, there was a paradigmic shift in thinking as researchers began to appreciate that TLE involved regions outside the ipsilateral hippocampus. One of the first novel methods involved analyzing volumes of manually segmented brain structures in the temporal and extra- temporal regions. Quantitative volumetric studies found atrophy in the neocortex of the temporal lobe (Lencz et al., 1992), entorhinal cortex (Bernasconi et al., 1999, 2003), parahippocampal gyrus (Bernasconi et al., 2003), fornix (Kuzniecky et al., 1999), and amygdala (Bernasconi et al., 2003; Salmenperä et al., 2001). When analyses were expanded to include extra-temporal regions, abnormalities were found in the basal ganglia (Decarli et al., 1998; Dreifuss et al., 2001), thalamus (Decarli et al., 1998; Szabo et al., 2006; Natsume et al., 2003), and cerebellum (Sandok et al., 2000; Hermann et al., 2005). To understand the clinical significance of the widespread anatomical irregularities with respect to cognitive function in patients with TLE, Hermann et al. (2003) found total white matter volume, but not total gray matter volume, to associate significantly with verbal memory function and other neuropsychological performance. Patients with TLE were also found to have greater white matter atrophy than gray matter atrophy compared to controls (Hermann et al., 2003). Given these findings, it was hypothesized that reduced white matter volume could result in disrupted cortico-cortical connectivity among eloquent brain regions, causing deficits in neuropsychological performance. However, it soon became evident that volumetric MRI was limited in its ability to characterize the vast pathology that co-exists in many TLE patients. Therefore, more advanced imaging protocols were necessary to detect microstructural white matter changes and resulting cortical disconnectivity in TLE.

1.3 Diffusion Tensor Imaging

Diffusion MRI was first introduced in the early 1980s as an extension of nuclear magnetic resonance (NMR) imaging to encode molecular diffusion effects in live tissue using magnetic field gradient pulses (Le Bihan, 1991). Diffusion, also known as Brownian motion (Einstein, 1905), is the random translational motion of molecules. One of the main advantages of diffusion MRI over structural MRI is that by modeling the diffusion of molecules (i.e. water), we are in effect, probing tissue structure at a microscopic scale that is much more fine-grained than conventional methods (Le Bihan et al., 2001). Being able to visualize water diffusion in live tissue like the brain has many clinical applications, with one of the first being in brain ischemia in the early 1990s (Warach et al., 1992). Also, since diffusion is a three-dimensional process and tissues may not be permissive to diffusion in all three axes equally, certain diffusion directions are favored over others. For example, water molecules will preferentially diffuse parallel to the direction of axon bundles rather than orthogonally (Basser et al., 1994). This diffusion anisotropy can then be measured by changing the direction of the gradient pulses and observing the change in the diffusion signal.

Diffusion anisotropy was formalized into an elegant model involving the diffusion tensor by Basser et al. (1994). The diffusion tensor describes the behavior of water diffusion as a 3-dimensional ellipsoid, mathematically represented as a 3x3 matrix, and diagonalization of the tensor yields a set of eigenvalues ($\lambda_1, \lambda_2, \lambda_3$) and eigenvectors ($\varepsilon_1, \varepsilon_2, \varepsilon_3$) (Alexander et al., 2007). From these eigenvalues, different diffusion metrics such as fractional anisotropy (FA) (Pierpaoli and Basser, 1996) and mean diffusivity (MD) can be calculated. FA is a scalar value from 0 to 1 that indicates the degree of diffusion anisotropy, while MD describes the amount of total isotropic diffusion within a defined space. Histological validation of these diffusion metrics in the rat brain have provided significant

evidence that reduced FA and increased MD correlate with axonal loss and demyelination in patients with neurological diseases (Budde et al., 2011; Lin et al., 2001), though FA has been used most often in DTI analysis and tractography.

1.3.1 Diffusion Tensor Imaging in TLE

In the past decade, many studies have emerged demonstrating reduced FA and increased MD in patients with epilepsy at the whole brain level. A recent systematic review and meta-analysis of the TLE literature including 2149 subjects with generalized epilepsy, frontal lobe epilepsy, TLE, and benign epilepsy with centro-temporal spikes, found whole brain FA in TLE to be significantly lower and whole brain MD to be significantly higher than controls (Slinger et al., 2016). Furthermore, they found that both increased MD and decreased FA were significantly correlated with earlier age of onset, longer duration of illness, and male sex in TLE (Slinger et al., 2016). This meta-analysis confirms previous findings by Hermann et al. (2003) to show white matter abnormalities exist and these can be detected at the whole brain level. However, using whole-brain diffusion measures may overlook and average out localized white matter atrophy that may otherwise be detected using more sophisticated white matter tractography algorithms.

To identify more fine-grained changes in white matter integrity in TLE, diffusion metrics in individual white matter tracts have been analyzed. Early tract-based analyses limited their scope to the limbic system and found increases in the apparent diffusion coefficient, a measure similar to MD, within the ipsilateral hippocampus and parahippocampus to correlate with poorer verbal memory performance (Lui et al., 2005). These early findings were extended to include other white matter tracts connecting temporal to extra-temporal regions. Specifically, impairment in delayed memory was found to correlate with diffusion abnormalities in the uncinate fasciculus (fronto-temporal tract) (Riley et al., 2010; McDon-

ald et al., 2008; Diehl et al., 2008), inferior longitudinal fasciculus (temporal- occipital tract) (McDonald et al., 2008; Riley et al., 2010), and inferior frontal occipital fasciculus (fronto-temporal-occipital tract) (McDonald et al., 2008). In summary, the collective MRI literature in TLE paints a compelling picture that TLE is a network disease affecting regions not just locally within the MTL, but also connectivity in many other parts of the brain. Diffusion tractography has generally focused on tracking large-scale white matter fiber bundles that do not allow for more fine-grained analyses of specific cortico-cortical connectivity. As a result, researchers have started to augment their neuroimaging toolbox with additional methods to scrutinize abnormal brain connectivity in TLE that may not be quantified with tract-based measures alone.

1.4 Connectomes

The conceptualization of the brain as a weighted graph (i.e. brain connectome) in which nodes (i.e. cortical regions) are interconnected to varying degrees (i.e. cortico-cortical connections) was first introduced by Sporns et al. (2005). The main hypothesis underlying all brain connectome analyses is that the structure defines the phenotypic expression of human cognition and behavior (Sporns et al., 2005). According to this hypothesis, any change to the underlying brain structure should produce evident changes in brain functioning. A recent meta-analysis of 26 neurodegenerative diseases including Alzheimer's, schizophrenia, and TLE found that network hubs (i.e. brain regions with large numbers of connections to other regions) were preferentially affected (Crossley et al., 2014). The authors further found that in nine of the disorders, including right and left TLE, median degree of lesion voxels was greater than that of non-lesion voxels (Crossley et al., 2014). In other words, lesions seemed to occur more frequently in network hubs like the hippocampus, thalamus, and anterior cingulate cortex than in other parts of the brain which

are not as interconnected. From this observation, a question arises: can we predict cognitive changes in TLE based on differences in their brain connectome properties?

Connectomes have been used to predict a myriad of neurological diseases, psychological disorders, and clinical variables in subjects (Brown and Hamarneh, 2016). It is important to understand the two main classes of connectomes in use. The first is based on functional connectivity, in which either resting-state or task-based fMRI data are used to find brain regions whose activity covary and generate connection matrices. The other is based on diffusion MRI, with which tractography is used to determine the extent to which two brain regions are anatomically connected to generate the connection matrices. Machine learning techniques have been applied to connectome data to predict clinical diagnoses for patients with schizophrenia (Dodero et al., 2015; Arbabshirani et al., 2013; Shen et al., 2010), major depressive disorder (Craddock et al., 2009; Rosa et al., 2013; Sacchet et al., 2015), attention deficit-hyperactivity disorder (ADHD) (Cheng et al., 2012), and bipolar disorder (Moyer et al., 2015). In terms of clinical variables, Rosenberg et al. (2015) used functional connectivity to predict individual differences in performance during an attention fMRI task in an ADHD population. One major downside of functional connectivity is that it does not capture true anatomical connections between two brain regions. Just because two regions covary over a period of time does not mean that they are connected and communicate directly with each other. For example, there may be a third region that is confounding the measurements by influencing the behavior of both regions. It is for this reason that I will only focus on studies that use structural connectivity in the context of TLE.

In the TLE literature, the focus of connectome-based modeling has mainly been to predict post-operative seizure freedom. Bonilha et al. (2015) calculated the degree to which a subject's structural connectome was abnormal relative to controls and used that

to predict seizure freedom after ATL. The authors also found ipsilateral connections in the temporal lobe to be important in this classification paradigm, something that has been replicated in other studies as well (Bonilha et al., 2015; Taylor et al., 2018a; Gleichgerrcht et al., 2018). These studies have demonstrated good classification performance, ranging from 79% (Taylor et al., 2018a) to 88% (Bonilha et al., 2015). However, no studies to date have used the structural connectome to predict memory impairments in patients with TLE. This is of high importance because using the structure connectome to identify *pre*-operative networks that underlie memory impairment in TLE could help to inform how (and when) ATL or other surgical procedures lead to further memory decline.

1.5 Current study

In this study, we used a machine learning algorithm (*XGBoost*) to predict memory impairment status in AED-resistant TLE patients using structural connectomes. A multi-site dataset was used to test the generalizability of our results. A secondary goal was to compare the predictive ability of the structural connectome analysis to conventional tract-based analysis and HCV. We hypothesized that the connectome analysis could provide more individualized connectivity differences that would lead to better classification performance relative to the tract-based and HCV analyses. Finally, we analyzed and report the most predictive features from each of the models to improve neuro-anatomical interpretability of the models.

2 METHODS

2.1 Subjects

This study was approved by the Institutional Review Boards at the University of California, San Diego (UCSD) and University of California, San Francisco (UCSF). All participants provided informed consent according to the Declaration of Helsinki. Eighty-one patients with medically refractory TLE had volumetric MRI, DTI, clinical data, and neuropsychological testing that allowed for inclusion in the study. All patients were under evaluation for surgical treatment at UCSD and UCSF Epilepsy Centers. Inclusion criteria included a diagnosis of medically refractory TLE by board-certified neurologists with expertise in epileptology and age between 18-55. Patients were classified into left TLE (LTLE; N=41), right TLE (RTLE; N=35), or bilateral TLE (N=5) based on seizure onsets recorded by video-EEG telemetry, seizure semiology, and neuroimaging results. Where clinically indicated, patients underwent Phase II video-EEG monitoring using foramen ovale or depth electrodes to confirm temporal lobe seizure onset. Clinical MRI scans were available on all patients (i.e. T1-weighted, T2-weighted, and coronal FLAIR sequences with 1mm slices through the MTL). MRIs were visually inspected by a board-certified neuroradiologist for detection of mesial temporal sclerosis (MTS) and the exclusion of contralateral temporal lobe structural abnormalities. MRI findings suggested presence of ipsilateral MTS in 41 patients. Patients were excluded if there was evidence of large

structural lesions or extra-hippocampal pathology on clinical MRI, current substance abuse, or history of significant psychiatric co-morbidity requiring hospitalization. Sixty-one control subjects were recruited for the study that were sex- and age-matched to the patient population. Control patients were excluded if there was any evidence of neurological or psychiatric condition, or a learning disability.

2.2 Neuropsychological testing

Neuropsychological testing was available for all patient and control subjects. Verbal memory was assessed using the California Verbal Learning Test-Second Edition (Delis et al., 2000) (CVLT) long delay free recall, Wechsler (Wechsler, 1997) Memory Scale-Third Edition logical memory delayed, and verbal paired associates (VPA) delayed (Wechsler, 1997). Raw scores were used to determine impairment status. For each test, z-scores were calculated for each patient relative to the distribution of controls, and patients with z-scores under -1.5 were classified as impaired for that specific test. As described by Edmonds et al. (2016), patients were classified as "memory impaired" if they were impaired on at least two out of three tests. Fifty-four percent of patients from UCSD were memory impaired, while 64% of patients from UCSF were impaired. All other patients were classified as "not impaired."

2.3 MRI acquisition

All patients were seizure-free per self-report for a minimum of 24 hours prior to the MRI scan. Brain imaging for all subjects was performed on a General Electric Discovery MR750 3T scanner with an 8-channel phased-array head coil at the Center for Functional MRI at UCSD or the Surbeck Laboratory for Advanced Imaging at UCSF.

Image acquisitions were identical at both centers and included a conventional three-plane localizer, GE calibration scan, a T1- weighted 3D structural scan (TR = 8.08 msec, TE = 3.16 msec, TI = 600 msec, flip angle = 8°, FOV = 256 mm, matrix = 256 x 192, slice thickness = 1.2mm; resampled to 1mm isotropic), and a single-shot pulsed-field gradient spin-echo EPI sequence (TE/TR = 96 ms/17 s; FOV = 24 cm, matrix = 128x128x48; axial). Diffusion images were acquired with b = 0 and b = 1000 mm^2/s with 30 diffusion gradient directions. Two additional b = 0 volumes were acquired with either forward or reverse phase-encode polarity for use in nonlinear B_0 correction.

2.4 DTI processing

The diffusion weighted images (DWI) were first corrected for distortions due to magnetic susceptibility (B_0), eddy currents, gradient nonlinearities, and head motion. The DWIs were then co-registered to the respective T1-weighted structural images. A reverse gradient method was used for the B_0 correction (Holland et al., 2010). This method provides superior accuracy and better cross-modality registration relative to the field mapping approach. A detailed description of the image processing is provided elsewhere (McDonald et al., 2014). The DTI-derived measure of FA was calculated from a tensor fit to b = 1000 data.

2.5 Fiber tract calculations

Fiber tract values were derived using a probabilistic diffusion tensor atlas created using in-house software written in C++ and MATLAB (i.e. AtlasTrack). A full description of the atlas and the steps used to create the atlas are given elsewhere (Hagler et al., 2009). For each subject, the T1-weighted structural images were nonlinearly registered to a common

space and the respective diffusion tensor orientation estimates were compared to the atlas. This resulted in a map of the relative probability that a voxel belongs to a particular tract given its location and similarity of diffusion orientation. Voxels identified with automated brain segmentation software (i.e. Freesurfer v5.3) as CSF or gray matter were excluded from the fiber regions of interests (ROIs). Average diffusion metrics were calculated for each fiber ROI, weighted by fiber probability, so that voxels with low probability of belonging to a given fiber contributed minimally to average values. In the current study, this probabilistic atlas-based method was used to reconstruct the following right and left hemisphere temporal lobe fiber tracts due to evidence of their disruption in TLE and likely involvement in memory processing (Diehl et al., 2008; McDonald et al., 2008; Riley et al., 2010): fornix (FX), parahippocampal cingulum (PHC), uncinate fasciculus (UNC), inferior longitudinal fasciculus (ILF), inferior frontal occipital fasciculus (IFOF) (Figure 1).

2.6 Volumetrics

Automatic segmentation of the right and left hippocampi was performed with Freesurfer (v5.3) using the structural T1-weighted images. The segmentations were visually inspected to ensure correct labeling of the hippocampus. Left and right HCV were calculated by counting the number of voxels in the segmentations. Intracranial volume (ICV) was calculated for each subject by first running BET (i.e. brain extraction tool Smith, 2002) on each T1-weighted image and counting the number of extracted voxels. HCVs were adjusted for head size by dividing by the ICV for each subject.

2.7 Structural connectome generation

The FMRIB Diffusion Toolbox (FDT), which is part of the FMRIB Software Library (FSL), was used for local diffusion modeling and performing the connectome-based tractography (Behrens et al., 2003, 2007). Probabilistic tractography was performed to calculate connection strength values between cortical regions corresponding to those from Freesurfer's Desikan-Killiany (DK) atlas. The cortical ROIs were obtained using Freesurfer's automatic parcellation process applied to each T1-weighted image. These connection strength values were then compiled into 2-D symmetric *n*x*n* matrices to yield brain connectomes for each subject.

Probabilistic fiber tracking was performed using FDT. A GPU-accelerated implementation of FDT's BEDPOSTX was run to estimate the diffusion parameters at each voxel of the DWIs (Hernández et al., 2013). Briefly, BEDPOSTX employs Markov Chain Monte Carlo sampling to calculate distributions on diffusion parameters at each voxel, while also accounting for crossing fibers within each voxel. The full description of the sampling and crossing fiber models can be found elsewhere (Behrens et al., 2003, 2007). Probabilistic tractography was then performed using FDT's PROBTRACKX2 with the following parameters: 5000 samples, 2000 steps per sample, 0.5 mm step length, 0.2 curvature threshold, loop checking enabled on paths. Path distributions were also corrected for the inherent linear bias towards longer pathways in tractography algorithms (Hagmann et al., 2007). A GPU-accelerated implementation of PROBTRACKX2 was used to take advantage of parallel computation (Hernandez-Fernandez et al., 2016). PROBTRACKX2 generates connectivity distributions from user-specified seed regions, in which voxels in the output brain image have values representing the number of streamlines (i.e. connection strength values) passing through them from the specified seed region. A full description of FDT's tractography implementation can be found elsewhere (Behrens et al., 2003, 2007).

The cortical seed regions fed to PROBTRACKX2 were acquired from Freesurfer's automatic cortical parcellation and segmentation process applied to T1-weighted images. This parcellation algorithm uses probabilistic information estimated from manually segmented brains (i.e. training set) to label each location on the cortical surface, incorporating geometric information derived from the cortical model and neuroanatomical conventions extracted from the training set. The resulting parcellation covers all sulci and gyri of the brain. The initial parcellation was performed with the Desikan-Killiany atlas yielding 70 total ROIs (35 per hemisphere). To create more fine-grained ROIs, the following DK ROIs were split orthogonally to the long axis of the parcellation: middletemporal, superiortemporal, inferiortemporal, fusiform, postcentral, precentral, rostralmiddlefrontal, and superiorfrontal. The rostralmiddlefrontal parcellation was split into two ROIs, while the rest were split into three ROIs. The resulting atlas contained 98 ROIs (49 for each hemisphere). The cortical segmentations were transformed from Freesurfer's conformed space to each subject's diffusion space using an affine transformation performed with FSL's FLIRT. Tractography was performed from each source ROI i and processed to calculate the connectivity distributions to every other destination ROI j, with self loops set to 0. To create a 98x98 symmetric connectivity matrix, the connectivity from $\text{ROI}_i \rightarrow \text{ROI}_j$ and $\text{ROI}_j \rightarrow \text{ROI}_i$ were averaged. These connectivity values were also normalized by the sum of the number of voxels of the source and destination ROIs to account for differences in head size between subjects.

2.8 Classification Model

In this study, XGBoost (v0.81) was used for all classification tasks. XGBoost is a type of decision tree algorithm that is widely used in many machine learning tasks (Chen and Guestrin, 2016). Similar to other such decision tree models as random forest, XGBoost

constructs many shallow trees (i.e. weak learners) that each by themselves, do not provide good classification results. However, by ensembling these weak learners, it is possible to achieve good classification performance. XGBoost improves upon the random forest algorithm by using gradient boosting to minimize the training error, thereby focusing on the mistakes made by the previous trees and correcting the internal model to account for these outliers. Furthermore, XGBoost introduces regularization terms to limit the depths of the weak learners and penalize the L2 norm of the cost objective. These regularization terms protect against overfitting to the training data by making the model more conservative and simple. XGBoost was chosen as the classification model for this study because it is theoretically more robust to potential outliers that may exist in our relatively small dataset.

2.9 Memory Impairment Prediction Model with Connectomes

The memory impairment prediction paradigm was designed as follows: 1) The dataset was split into UCSD (i.e. training set) and UCSF subjects (i.e. testing set) 2) principal component analysis (PCA) was performed on the training set to learn the transformation parameters 3) the training and testing sets were transformed using the aforementioned PCA parameter matrix 4) the training and testing sets were scaled to zero mean and unit variance 5) XGBoost was trained on the training set and 6) performance on the testing set was evaluated. See Figure 2 for a visual representation of the prediction pipeline.

PCA was performed on the connectome data to reduce dimensionality of the input data. PCA is an unsupervised learning algorithm that finds a set of eigenvectors onto which the original data can be mapped with minimal loss of variability. In other words, PCA finds the directions in which the observations have most the variance and thus, most differentiate

the data. These directions are known as the principal components (PCs) that can then be used in various supervised machine learning tasks like classification. The number of PCs that yielded maximum accuracy was assessed through hyperparameter optimization. Hyperparameter optimization involves systematically tuning the internal parameters of the machine learning model to arrive at a set of parameters which yield maximum performance.

Because the connectomes were symmetric across the diagonal, the upper triangles were extracted, resulting in 4753 connections (i.e. features) per subject. Also since TLE has been shown to affect connectivity within the temporal lobe and temporal to extratemporal regions (Besson et al., 2014) and these connections are likely critical to memory (Bonilha et al., 2007; Voets et al., 2014), only connections starting or ending in the temporal lobe were kept. Hyperparameter optimization was performed to tune the performance of all the models. It was found that having 10 PCs maximized accuracy of the connectome model. These 10 PCs explained 68% of the variance of the original dataset. No cross validation was performed, as an external dataset was available for testing. Performance was evaluated with receiver operating characteristic (ROC) curves, area under the curve (AUC), accuracy, positive predictive value (PPV), negative predictive value (NPV), sensitivity, and specificity. The thresholds for the predictions were chosen based on the point on the ROC curve that yielded highest accuracy.

Definitions for the performance metrics will reference Figure 3. Suppose a classifier selects some elements to be of the positive class and the rest to be negative. We can then calculate the number of true postives (TP), true negatives (TN), false positives (FP), and false negatives (FN). From these, PPV, NPV, sensitivity, and specificity can be calculated

as such.

$$PPV = \frac{TP}{TP+FP}$$
$$NPV = \frac{TN}{TN+FN}$$
$$Sensitivity = \frac{TP}{TP+FN}$$
$$Specificity = \frac{TN}{TN+FP}$$

2.10 Classification model employing other features

Additional models were tested using the following combination of features: clinical variables, HCV, tract FA values (Tract), Tract + HCV, and Connectome + HCV. Clinical variables included age, education, sex, handedness, MTS status, side of epileptic onset, age of onset, number of anti-epileptic drugs (AEDs), and seizure frequency. The same prediction paradigm as with the connectome data was followed, with the exception that PCA was not performed with non-connectome data since these data were not high dimensional. Categorical clinical variables, such as MTS status and sex, were binarized. Left and right HCVs were normalized to total intracranial volume to correct for head size and included in the respective models. Hyperparameter optimization was performed on every set of models constructed to maximize their performance.

2.11 Randomization testing

Randomization testing was done to assess statistically significant differences in performance between different models. A distribution of performance metrics was generated by repeatedly training the model on a subset of the training set and testing on the whole

testing set. During each iteration, two training subjects were randomly removed such that 46 training subjects (instead of 48) were available. Then, the model performed predictions on the entire testing set (i.e. 33 subjects). This process was repeated 1000 times and the means and standard deviations of each performance metric for each model were collated.

2.12 Linking principal components from PCA to biological underpinnings

To connect the PCs back to connectivity changes in TLE, further analysis was performed. Mathematically, PCs are computed as linear combinations of the original features

$$\mathrm{PC}^j = \sum_{i=1}^{N} \beta_i^j X_i \tag{2.1}$$

where PC^j is the j-th principal component, X_is are the original features, and β_is are the corresponding weights. In this study, the original features were temporal subnetwork connections from the upper triangles of the connectomes. A connection was deemed to be important if its corresponding weight was large ($>$0.10) in absolute value. A weight matrix for the PCs was extracted and the most important connections contributing to each PC were found. The most important connections were those with the highest weight and were interpreted to be connections most important for differentiating memory impaired from non impaired subjects.

The connection weight matrix was further processed to determine which connections had preferentially greater influence on important PCs than non-important PCs. Feature importance values were extracted from the connectome model and demeaned. Following this, the demeaned feature importance values were scaled from -1 to 1, with -1 corre-

sponding to the least important PC and +1 corresponding to the most important PC. The connection weights for each PC were multiplied by the respective scaled feature importance values and sums were taken across each connection. Connections which contributed greatly to only important PCs would have more positive values, while connections that contributed equally to all PCs or greatly to only non-important PCs would have more negative values.

3 RESULTS

3.1 Patient Demographics and Clinical Variables

There were differences in education ($t(79) = -2.06, p \leq .042$) and age ($t(79) = -3.134, p = .002$) between the UCSD (training) and UCSF (testing) datasets with the UCSD patients having a higher mean level of education and older age. There were no differences in sex distribution (Fisher's Exact = .177, $p = .821$) between the two groups (Table 1).

In the training set, there were no differences in age (t(46) = -1.167, $p = .246$) , education($t(46) = .530, p = .598$), handedness (Fisher's Exact = 1.261, $p = .812$), age of onset ($t(46) = -.526, p = .602$), duration of epilepsy ($t(46) = -.488, p = .628$), seizure frequency ($t(45) = -.738, p = .465$), number of AEDs ($t(45) = -.484, p = .631$), MTS status (Fisher's Exact = 4.022, $p = .081$) or side of seizure onset (Fisher's Exact= .348, $p = 1.00$) between the Memory impaired and Not impaired groups. However, there were differences in sex distribution between the two groups (Fisher's Exact = 4.481, $p = .045$), with the Memory impaired group having a greater proportion of females.

In the testing set, there were no differences in age ($t(31) = -1.287, p = .208$), education ($t(31) = -.964, p = .343$), sex distribution (Fisher's Exact = .017, $p = 1.00$), handedness (Fisher's Exact = .614, $p = 1.00$), age of onset ($t(31) = -1.968, p = .058$), duration of epilepsy ($t(31) = 1.194, p = .241$), seizure frequency ($t(31) = -1.287, p =$

.208), number of AEDs ($t(31) = 1.540, p = .134$), MTS status (Fisher's Exact = .351, $p = .721$) or side of seizure onset (Fisher's Exact= 1.954, $p = .356$) between the Memory impaired and Not impaired groups.

3.2 Unimodal feature performance

Multiple XGBoost models were constructed for comparison of feature importance to predicting memory impairment. XGBoost models were trained with the following features: clinical variables, HCV, average FA of the temporal lobe white matter tracts (Tract), and connectome. The full results of model performance with these features are shown in Table 2. Randomization results from sampling 1000 times are given in Table 3. It is important to note that 64% accuracy is considered baseline performance (i.e.the performance of a classifier that predicts all subjects as memory impaired).

Neither the clinical model nor the HCV model performed better than baseline, with the clinical model yielding the poorest accuracy at 61%. The HCV model performed at 66% accuracy, which was slightly better than the clinical model ($p < 0.05$). The main gain in performance was realized when white matter-based features were used. The Tract and connectome models performed significantly better than the HCV ($p < 0.001$) and clinical models ($p < 0.001$), with the connectome model numerically outperforming the Tract model. However, the connectome model (76% accuracy) did not have significantly higher accuracy than the Tract model (73% accuracy).

It was interesting to note that the white-matter based models showed the highest PPV, that is, a positive prediction of memory impairment was likely to have been correct. Although the NPV of the HCV model shown in Table 2 is lower numerically than the white-matter based models, the HCV model performed significantly better in the NPV metric than the Tract ($p < 0.05$) and connectome models ($p < 0.05$) during randomization

testing. In terms of PPV, the connectome and tract models were indistinguishible from the HCV model but both were significantly better ($p < 0.05$) than the clinical model.

ROC curves were constructed to analyze the relationship between the specificity and sensitivity of each model. As seen in Figure 4, the ROC curve for the clinical model dips under the diagonal dashed line, indicating that it performs at baseline (AUC = 0.43). This is in contrast to the ROC curves for the connectome and Tract models, which have the highest AUCs and indicate that these models perform the best, with the connectome model (AUC = 0.71) similar to the Tract model (AUC = 0.68).

3.3 Multimodal feature performance

In order to test the added value of our two white matter models to HCV, we paired the Tract model with HCV (TractHCV) and the connectome model with HCV (ConnHCV). The ConnHCV model numerically out-performed the TractHCV model, with 81% accuracy and 0.82 PPV. The TractHCV and ConnHCV models both yielded 0.80 NPV; however, the TractHCV had the highest sensitivity of 0.95. Furthermore, these models did not perform signficantly better in any of the metrics presented than the respective models without HCV, suggesting HCV does not add new information to help white-matter models perform better. ROC curve analysis of both these models revealed the ConnHCV to have AUC of 0.76 and TractHCV model to have AUC of 0.72.

3.4 Important features from each model

To improve neuro-anatomical interpretability, feature importance values were extracted from each model. The five most important features from each model are plotted in Figures 6 and 7. The most important features for classifying memory impairment in

the clinical model included age of onset, seizure frequency, and age. Of note, even though MTS status is regarded clinically as an important risk factor for memory impairment, it did not emerge as one of the five most important features in this model (Figure 6a). Similarly, side of epileptic onset did not discriminate between memory impaired and not-impaired patients. Not surprisingly, left HCV emerged as more important than right HCV for verbal memory impairment prediction in the HCV model (Figure 6b).

In both the Tract and TractHCV models, the three white matter tracts contributing the most to memory impairment prediction were the left ILF, left UNC, and right PHC (Figures 6c, 7a). Bilateral tracts were found to contribute most to memory impairment prediction. It is of further interest that left HCV only emerged as the fourth most important feature in the TractHCV model. Additionally, the left ILF was consistently the most important tract for the classification in both tract-based models.

In the connectome model, the most important principal component (PC) towards memory impairment prediction was PC-6, followed by PC-7 and PC-10. A peculiar result from this is that the top 3 important PCs were those explaining the least amount of variance in the original data. When HCV features were added to the connectome model, the three most important features became PC-4, PC-10, and right HCV. In contrast to the unimodal model, XGBoost considered right HCV to better discriminate between memory impaired and not impaired than left HCV in the ConnHCV model.

3.5 Cortical connections contributing the most important PCs

The most important cortico-cortical connections for the top three PCs were found to be localized mainly to the anterior temporal lobe (Figure 8a). In addition, 32% of the

top 15 connections for each PC were connections originating from the entorhinal and parahippocampal cortices.

Figure 8 displays the PCs that were most important (PC-6), moderately important (PC-2), and not important (PC-9) for classifying memory impaired versus not impaired patients in the connectome model. The top 15 most important connections for each of these PCs were then analyzed, to determine if more important PCs were impacted more by anterior temporal lobe connections than not important ones. The most important connections for PC-6 appear to mostly be localized in the anterior temporal lobe, with connectivity to extra-temporal regions. Conversely, PC-9 seems to be impacted most by posterior temporal to extratemporal lobe connections.

Cortico-cortical connections that preferentially contributed to more important PCs were determined. Several left hemispheric connections emerged as important after controlling for PC feature importance (Table 4, Figure 9). Of note, the left hemispheric connection from the temporal pole to the rostral fusiform emerged as the most important cortical connection. Other top connections included left temporal pole to left rostral inferior temporal gyrus, left entorhinal cortex to left precuneus, and left entorhinal cortex to the left isthmus of the cingulate.

4 DISCUSSION

In this study, we used machine learning methods and white matter network analysis (i.e. structural connectomes) to predict verbal memory impairment in patients with drug-resistant TLE. We also compared the predictive ability of the structural connectome analysis to conventional tract-based analysis, HCV, and clinical variables. Overall, we found white matter integrity to be more informative of verbal memory performance than HCV or clinical variables, with the white-matter models achieving significantly higher accuracy scores. Contrary to our hypothesis, the connectome performed on par with the tract-based model. However, we assert that our connectome model may provide more specific information about abnormal connectivity contributing to verbal memory performance, as described below. A multivariate model incorporating both white-matter microstructure and volumetric features appears to be most informative, providing the highest sensitivity and specificity for determining memory-impairment in TLE (Table 3).

4.1 White matter integrity is more important than HCV and clinical features for verbal memory

We found both white-matter based models to outperform left and right HCV and clinical models in terms of classification accuracy (Tables 2 and 3). This result reflects

previous findings from our lab that white-matter based analyses provide better predictions of verbal memory scores than HCV and other morphometric analyses (McDonald et al., 2014). In this study, the authors compared the value of DTI measures in the context of left HCV to explain verbal memory performance and found that MD of the left ILF was a stronger predictor of verbal memory performance than left HCV. Here, we were able to replicate this finding when analyzing the features that best discriminated between memory impaired and not impaired subjects in the combined tract and HCV model. As seen in Figure 7a, FA of the left ILF contributed the most towards memory impairment prediction, with left HCV only emerging as the fourth most important feature in that model. Both abnormal MD and FA in the left ILF seem to be strong predictors of verbal memory performance, suggesting the white matter integrity in the left ILF is highly critical for preserving verbal memory performance in TLE.

Another peculiar finding was that the HCV model demonstrated high NPV, while the white-matter models had higher PPV (Table 3). The high NPV of the HCV model indicates that negative predictions should be interpreted with high confidence, while the higher numerical PPV of the white-matter based models indicates that we should have high confidence in positive predictions. These findings demonstrate that hippocampal volume and measures of white matter abnormalities may provide independent diagnostic information in pre-surgical TLE evaluation. Assuming this pattern holds for models predicting post-operative memory decline (i.e. positive prediction means memory will decline), it may be possible to implement a two-stage testing procedure. In the first stage, HCV, derived from T1-weighted imaging, can be used to determine if a patient will not have post-operative memory decline. For any positive prediction, additional diffusion MRI can be ordered and a white-matter based model can be used to obtain a more accurate prediction as to whether the patient will suffer from post-operative memory decline.

Furthermore, we found the clinical model to perform the worst among all the models tested. Seizure related variables like age of onset, seizure frequency, and number of AEDs were among the most important variables contributing to the clinical model performance (Figure 6a), but the clinical model failed to perform better than chance. It was quite surprising to see that MTS status was not an important predictor in the clinical model, given the existing literature (Helmstaedter et al., 1997; Hermann et al., 1992; Alessio et al., 2004) and clinical assumptions that MTS is a strong predictor of verbal memory performance. Our results mesh with previous findings of seizure-related variables not contributing additional variance to verbal memory performance (McDonald et al., 2014) or only exhibiting weak associations (Hermann et al., 2006). Patients with similar clinical and seizure characteristics may have vastly different underlying white matter microstructure, resulting in heterogeneous memory performance that cannot be accurately described with clinical variables alone. Although these clinical variables are frequently used to estimate risk of post-surgical memory decline, our results suggest it may be worthwhile to utilize models of white matter integrity as a diagnostic tool in the prediction of post-operative memory outcome in addition to clinical variables.

4.2 Connectome adds novel information to tract-based and volumetric analyses

The structural connectome-based analysis appeared to be numerically superior to the traditional tract-based analysis (Table 2); however, we did not find significant improvement in classification accuracy over tract-based features. Nevertheless, one of the major strengths of this study is that it is the first study, to our knowledge, to apply machine learning with connectomics data for predicting memory impairment in TLE. Numerous studies have

used machine learning in the context of predicting surgical outcome, lateralization of seizure onset, and epilepsy diagnosis for individual patients. While there is much research examining how imaging correlates with memory performance in TLE at a group level, no studies to date have used machine learning to predict verbal memory performance at an individual level. We believe this study is the first step to achieving personalized "memory connectomes" that could provide important information for predicting risk for post-operative memory decline following epilepsy surgery.

Using a rather simple feature selection approach with PCA, we were able to capture interesting patterns of network abnormalities present in memory impaired patients that enabled our connectomics approach to match the performance of well-estabished tract-based analyses. One unexpected finding from our connectome analyses was that right HCV emerged as an important feature in the combined ConnHCV model, whereas left HCV did not. The TractHCV model, however, showed left HCV as being a more important feature than right HCV. We hypothesize that the connectome captures information about the left hippocampus (e.g. integrity of efferent or afferent hippocampal fibers that co-vary with left HCV, but are not captured by the tract-based analysis) that would make left HCV redundant as a feature while enabling right HCV to add novel information to boost classification performance.

Deeper analysis of the PCs also uncovered cortical connections contributing preferentially to important PCs in the connectome model (Table 4). Among these connections were those involving regions often implicated in episodic memory and the larger memory network like the left precuneus (Shallice et al., 1994), left inferior temporal gyrus (Chen et al., 2016) and entorhinal cortex. We inspected the tractography output for these cortical connections and observed that these connections overlap with those that would have been included in our MTL fiber association tracts, including the the left ILF and left PHC

(Wakana et al., 2007). Thus, many of the important connections that emerged from our connectome model were likely a subset of those included in our large, MTL bundles known to be important for memory, leading to similar prediction accuracies of the two methods. The left ILF was consistently the most important tract in the XGBoost models (Figures 6c, 7a) for predicting verbal memory impairment. Additionally, abnormalities in the left PHC have been found to be associated with worse verbal memory performance (McDonald et al., 2008). Although the connectome-based analysis was not found to perform significantly better than tract-based analyses, it does seem to provide a better understanding of how abnormal deep white matter tracts affect the connectivity of specific cortical regions that play a role in verbal and episodic memory. The convergence of the two methods is also encouraging, as it demonstrates that the importance of MTL white matter networks for predicting memory performance is robust to the tractography method employed (i.e., connectome-based versus tract-based).

4.3 Strengths, limitations, and future directions

This study is the first, to our knowledge, to use structural connectome for predicting verbal memory impairment in patients with TLE. Another major strength is the use of an independent external dataset to cross validate our results. In our case, we trained the XGBoost model on patients from the UCSD Epilepsy Center and tested the model on patients from the UCSF Epilepsy Center. This paradigm reduces the risk of overfitting the model to the data by testing the model on patients that the model has never seen before. We also took additional steps throughout the study methodology to ensure XGBoost had no information about the testing dataset during the training phase. Third, relatively few studies have performed comparative analyses of connectome-based approaches with more established methods. We analyzed connectome-based predictive modeling in the context of

tract-based and HCV analyses in this study and found that connectome-based modeling has the potential to provide more granular information about abnormal cortico-cortical connectivity underlying verbal memory impairment than tract-based methods in TLE.

Despite these strengths, our study did have several limitations that should be noted. First, in order to derive our memory-impaired and not impaired TLE groups, we collapsed across three somewhat different measures of verbal memory. The three memory indices we used in this study involved delayed recall of prose, verbal associative recall, and word list recall. It is well known that prose recall and associative memory recruit more lateral and medial temporal lobe structures respectively (Saling, 2009), while list learning may rely more heavily upon the hippocampus (Hirni et al., 2013). By pooling results across tests, the model may have lost some specificity as to which temporal lobe structures and connections are associated with the different types of learning. However, by requiring patients to be impaired on at least two of the measures, we felt more confident in our labeling of a patient as memory impaired. Second, our sample size was relatively small in the context of performing machine learning. It is challenging to achieve reasonably good machine learning performance with sample sizes common in neuroimaging studies. Machine learning algorithms need many examples in the training data to be able to detect patterns and effectively perform predictions on unseen data. It is possible that with a larger sample size, our connectome-based model would have outperformed the tract-based model since inspection of Table 2 would suggest a pattern in this direction across most indices. However, our patient sample is relatively special, as they suffer from drug-resistant TLE and are surgical candidates for ATL and laser ablation therapy. Thus, we have the unique opportunity to study both pre-operative and *post*-operative imaging in these patients, along with neuropsychological performance pre- and post-surgery. Future research with a larger sample size of pre-surgical and post-surgical neuropsychological data will examine

if it is possible to use our connectome-based or tract-based models to estimate risk for postoperative decline. Further study is also needed to determine the best dimensionality reduction approach to connectome data. While PCA was used in this study, graph theory measures have proven to be effective in predicting seizure outcome (Taylor et al., 2018b) and in characterizing cognitive phenotypes in TLE (Reyes et al., 2019). Such an approach may yield better classification performance, especially if graph theory measures can separate memory impaired and not impaired patients more sharply.

4.4 Conclusion

In summary, our data demonstrate the importance of white matter networks for predicting verbal memory impairment in TLE. Importantly, both connectome-based and tract-based models showed higher accuracy than important clinical characteristics or HCV for classifying TLE patients as memory-impaired and not impaired. Although the connectome model did not outperform the tract-based model, it may provide more granular information regarding the importance of specific MTL connections to memory performance. Collectively, these data could provide critical information for estimating risk for memory decline following different surgical interventions.

This thesis, in full, is currently being prepared for submission for publication of the material. Balachandra, Akshara R.; Kaestner, Erik; Bahrami, Naeim; Reyes, Anny; Macari, Anna-Christina; McDonald, Carrie R. The thesis author was the primary investigator and author of this material.

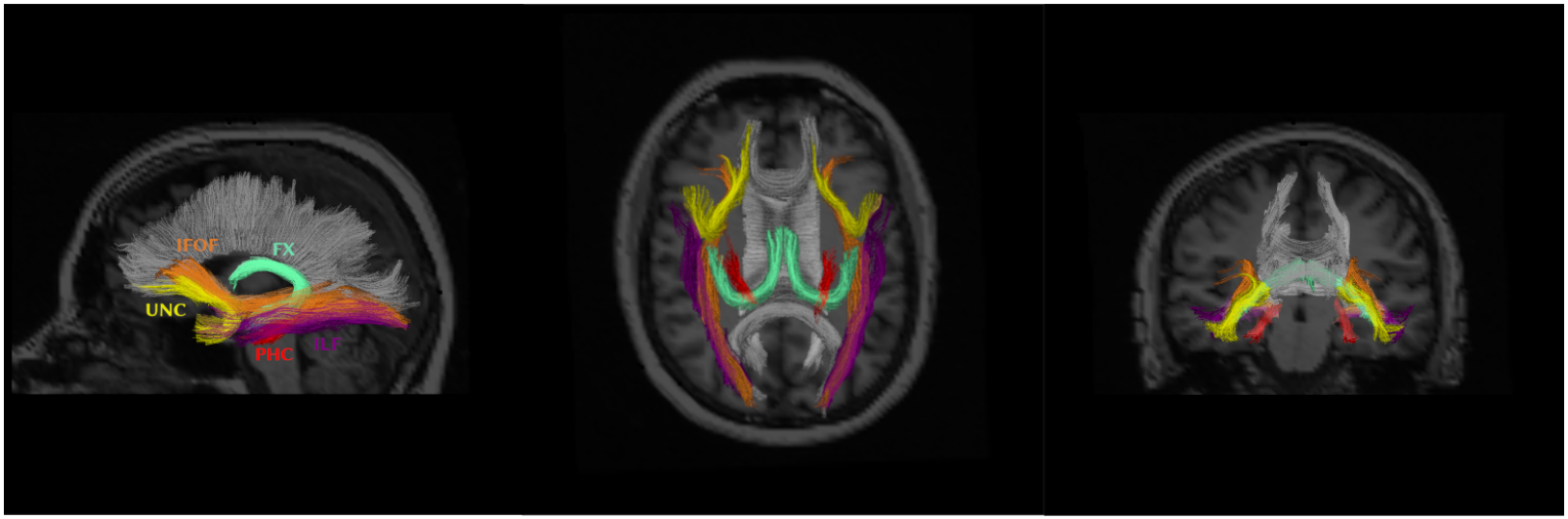


Figure 1: Deep white matter tracts of interest. Sagittal (left), axial (middle), and coronal (right) renderings of the fornix (FX), uncinate fasciculus (UNC), inferior longitudinal fasciculus (ILF), inferior frontal occipital fasciculus (IFOF), and parahippocampal cingulum (PHC) from AtlasTrack projected onto a T1-weighted image for a single individual. The corpus callosum is portrayed in light gray in order to provide additional spatial information.

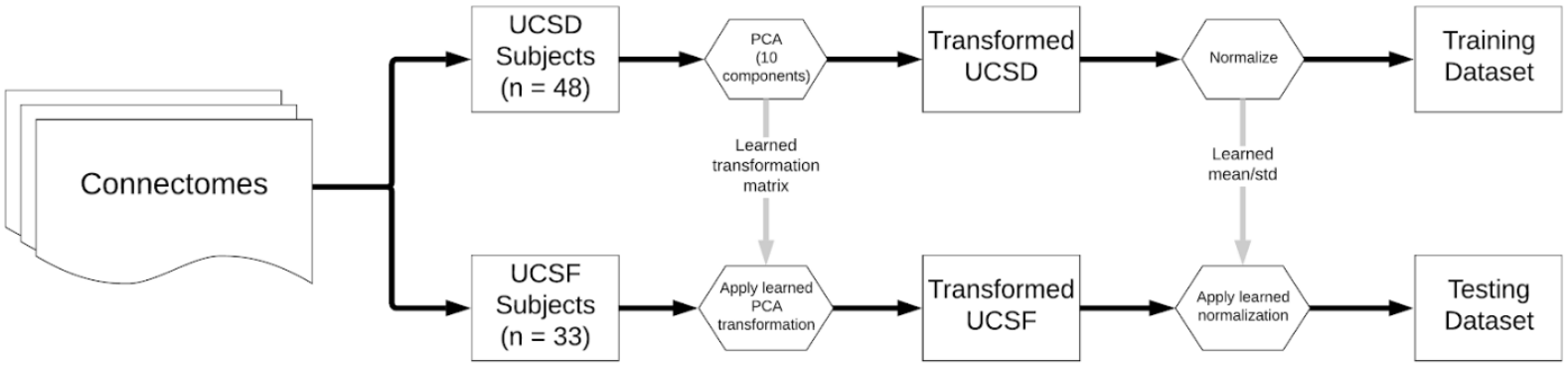


Figure 2: Connectome model pipeline illustrating the processing steps taken to reach the final training and testing datasets from the raw connectome matrices.

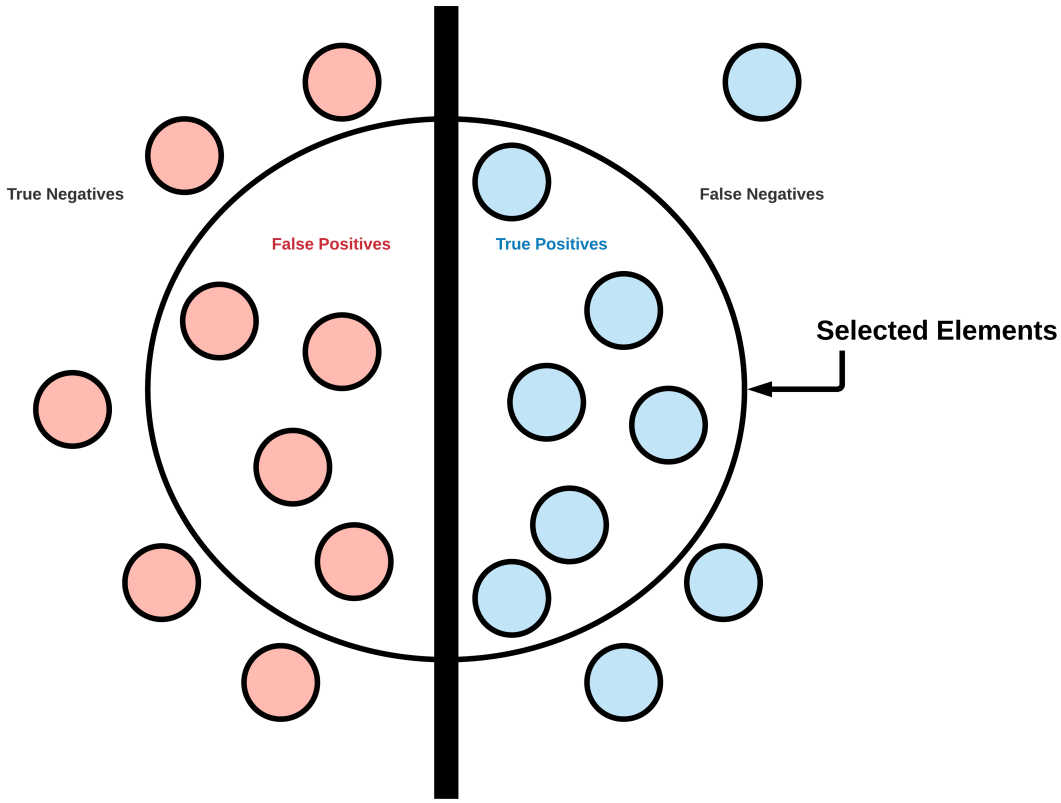


Figure 3: Sample classification model illustrating basic performance measures of machine learning models.

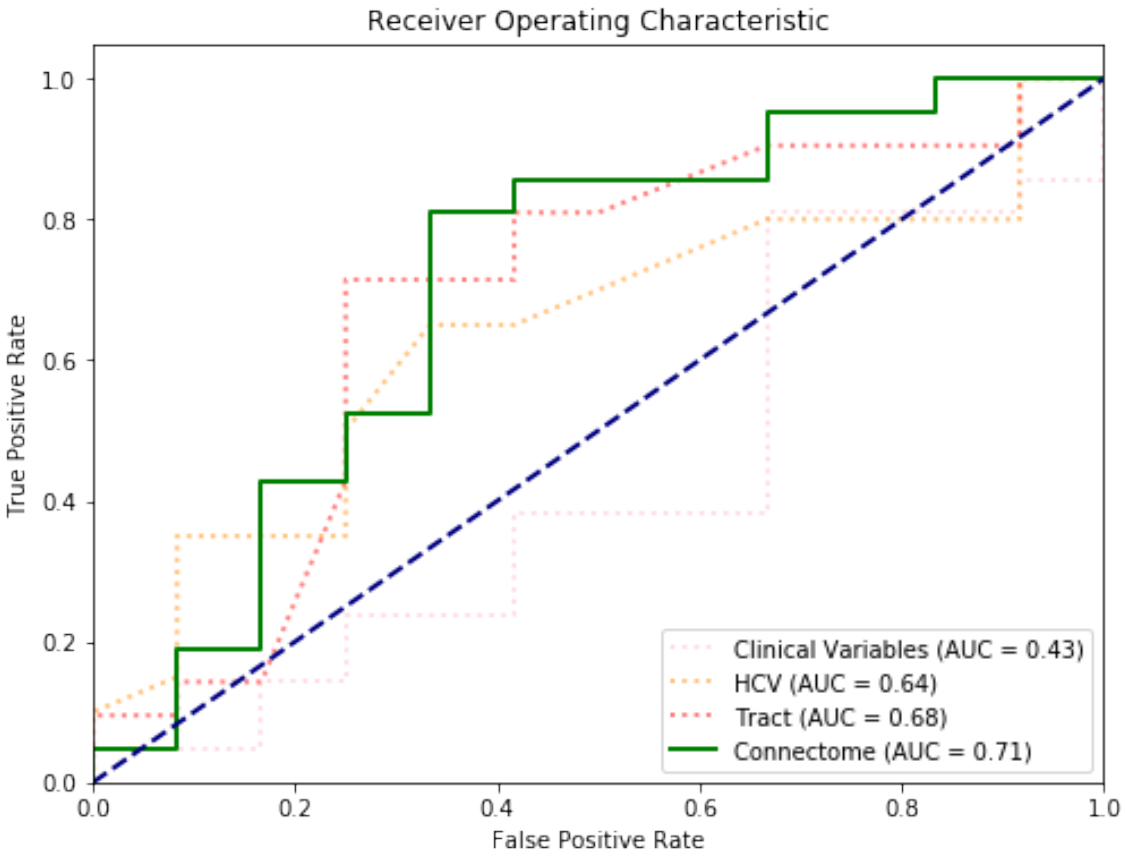


Figure 4: Unimodal features receiver operating characteristic (ROC) curves.

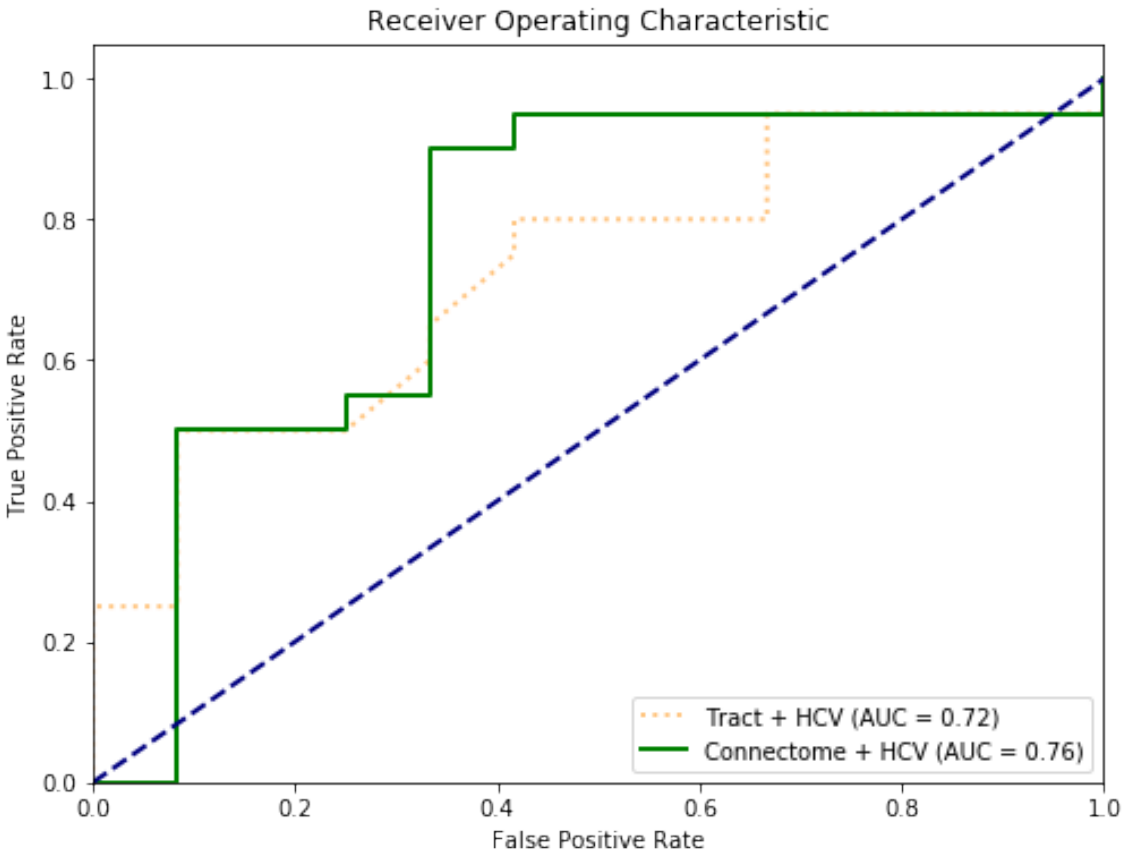
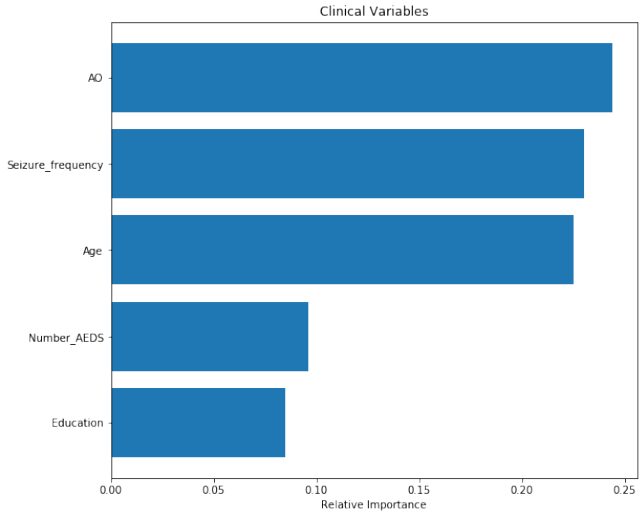
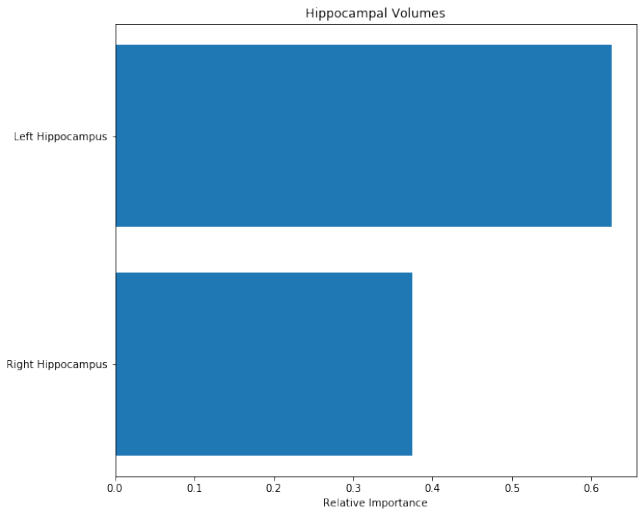


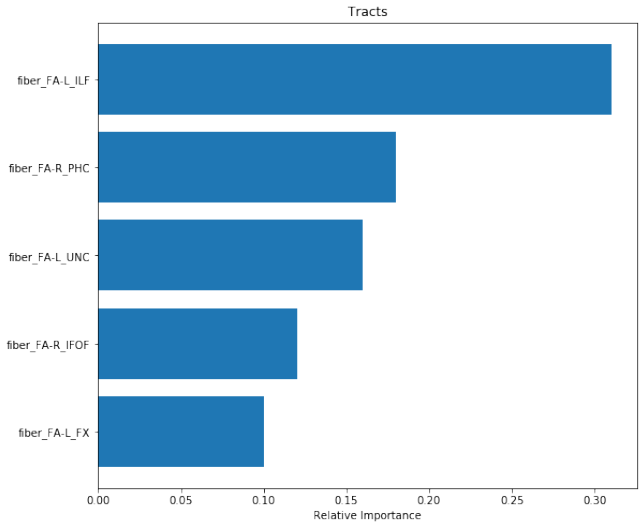
Figure 5: Multimodal features receiver operating characteristic (ROC) curves.



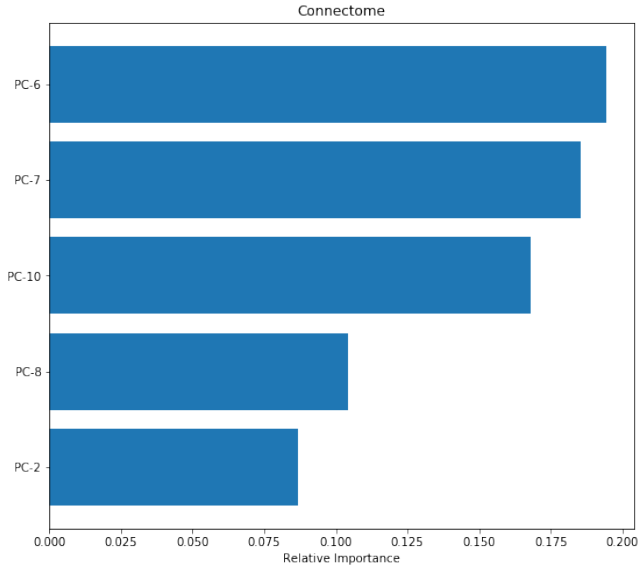
(a) Clinical feature importance



(b) Hippocampal volume feature importance

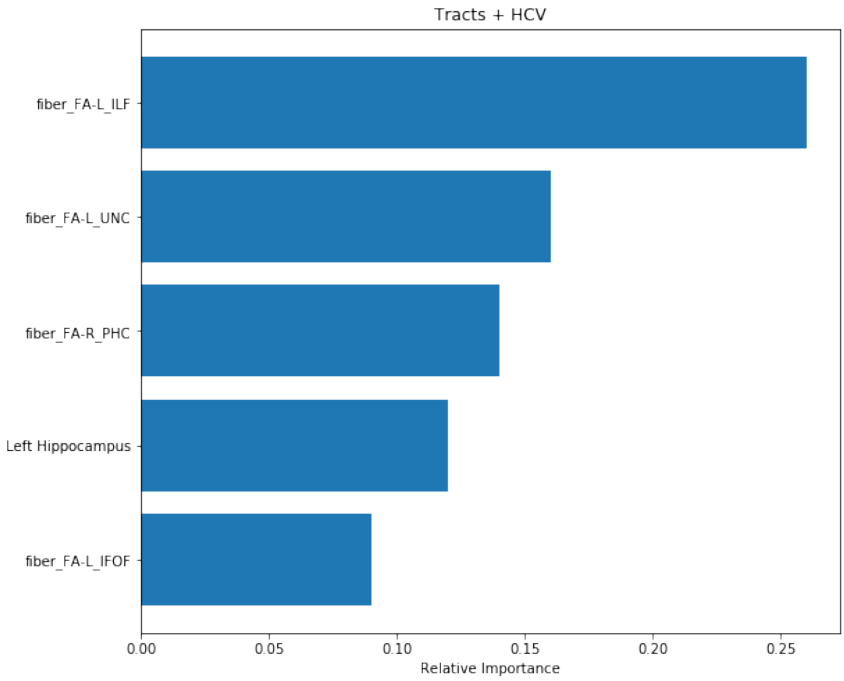


(c) Tract feature importance

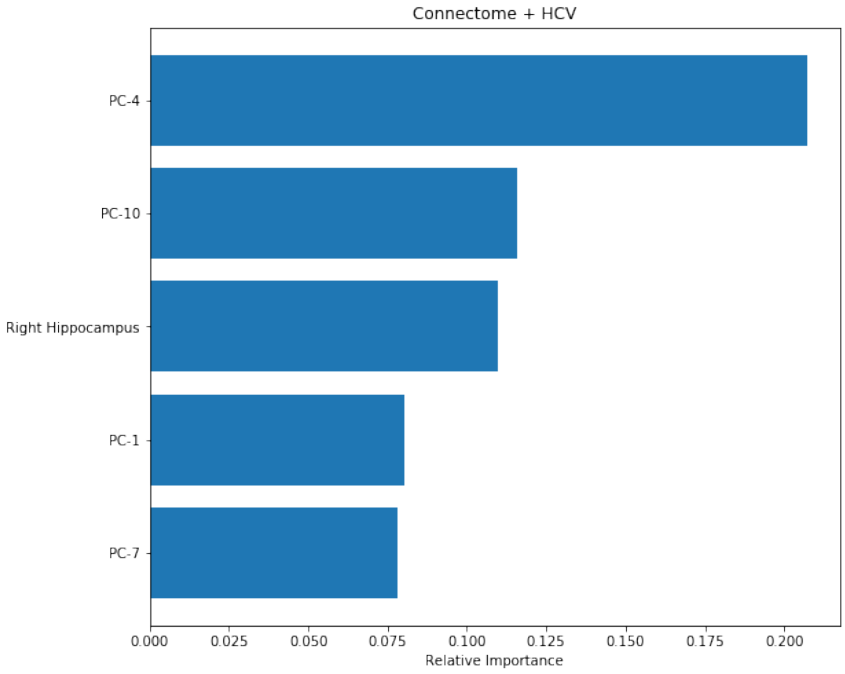


(d) Connectome (principal component) feature importance

Figure 6: Feature importance plots for each set of unimodal features.

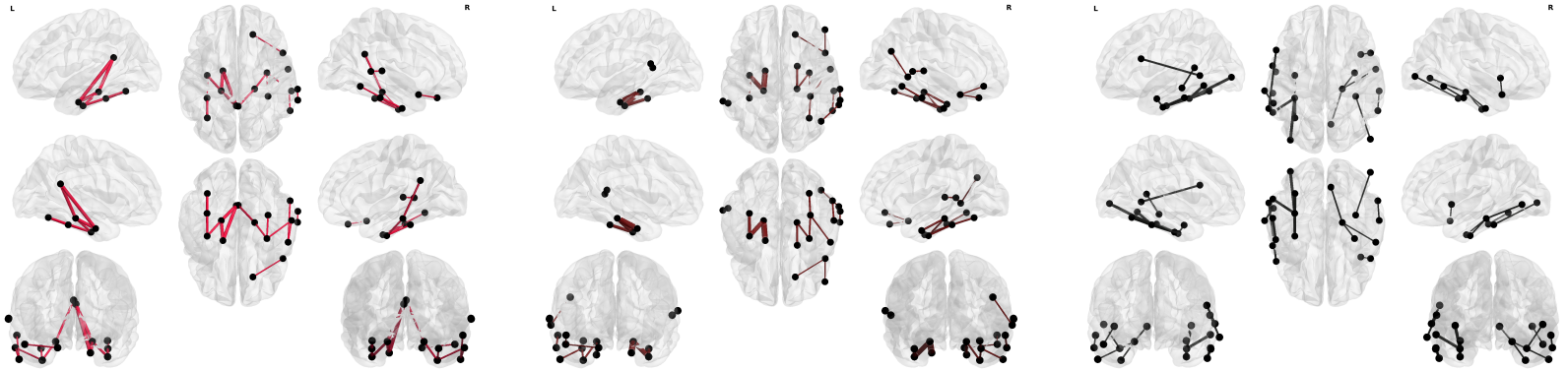


(a) Tract + HCV feature importance



(b) Connectome + HCV feature importance

Figure 7: Feature importance plots for multimodal prediction models.



(a) Connections with highest weight towards PC-6.

(b) Connections with highest weight towards PC-2.

(c) Connections with highest weight towards PC-9.

Figure 8: Connections with highest weight towards principal components. Red connections indicate those that had highest weight towards principal components that were found to better discriminate between memory impaired and not impaired subjects. Black connections indicate those with high weight towards PCs that did not contribute meaningfully to memory impairment prediction. Examples of PCs that were very important (PC-6), moderately important (PC-2), and not important (PC-9) are shown.

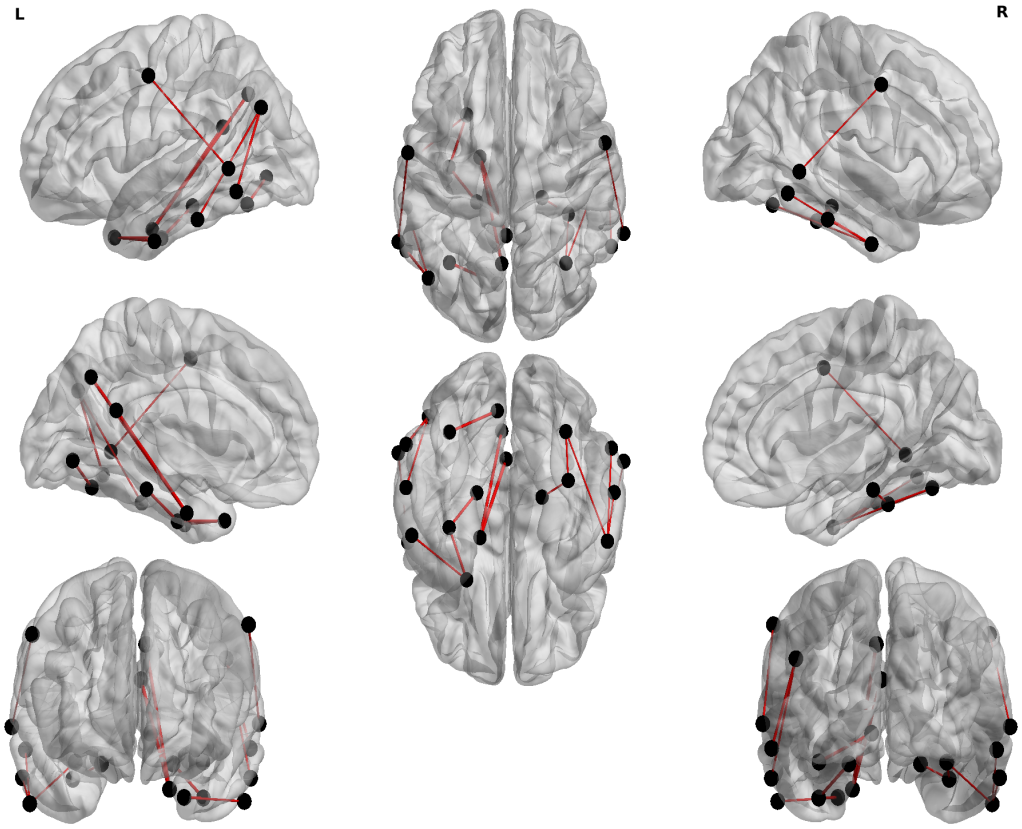


Figure 9: Top 15 most important connections for memory impairment classification. These connections contributed preferentially to the most important PCs

Table 1: Demographics and clinical variables. TLE: temporal lobe epilepsy; F: females; M: males; L: left; R: right; A: ambidextrous; MTS: mesial temporal sclerosis; AEDs: antiepileptic drugs; standard deviations are presented inside the parentheses

	Training Set		Testing Set	
N	48		33	
Age	39.71 (13.85)		30.72 (10.72)	
Education	14.08 (2.26)		13.09 (1.91)	
Sex: M/F	27/21		17/16	
	Memory Impaired	Not Impaired	Memory Impaired	Not Impaired
N	26	22	21	12
Age (years)	41.84 (15.68)	37.18 (11.14)	32.52 (11.66)	27.58 (8.36)
Education (Years)	13.92 (2.56)	14.27 (1.88)	13.33 (2.31)	12.67 (.77)
Sex: M/F	11/15	16/6	11/10	6/6
Handedness: L/R/A	2/23/1	3/19/0	2/18/1	1/11/0
MTS: Yes/No	17/9	8/14	11/10	5/7
Side: L/R/Bilateral	12/12/2	10/11/1	14/6/1	5/6/1
Age of Onset	23.11 (17.30)	20.82 (11.91)	22.67 (11.53)	13.58 (14.71)
Duration (years)	18.73 (17.52)	16.36 (15.75)	9.86 (9.93)	14.00 (8.93)
Number of AEDs	2.4 (.86)	2.27 (.93)	2.1 (.91)	2.67 (1.15)
Seizure frequency	12.38 (25.62)	7.91 (13.07)	11.05 (19.02)	3.83 (4.23)

Table 2: XGBoost model performance with each set of features. PPV = Positive Predictive Value; NPV = Negative Predictive Value; AUC = Area Under the Curve

	Accuracy	PPV	NPV	Sensitivity	Specificity	AUC
Clinical Variables	0.61	0.67	0.44	0.76	0.33	0.43
HCV	0.66	0.76	0.53	0.65	**0.67**	0.64
Tracts	0.73	0.77	0.64	0.81	0.58	0.68
Connectome	0.76	0.81	0.67	0.81	**0.67**	0.71
Tracts + HCV	0.72	0.7	**0.8**	**0.95**	0.33	0.72
Connectome + HCV	**0.81**	**0.82**	**0.8**	0.9	**0.67**	**0.76**

Table 3: Distribution of metrics with randomization testing for each machine learning model.

	Accuracy	**PPV**	**NPV**	**Sensitivity**	**Specificity**
Clinical Variables	0.62 ± 0.02	0.66 ± 0.02	0.37 ± 0.25	0.85 ± 0.09	0.21 ± 0.16
HCV	0.66 ± 0.01	0.69 ± 0.06	0.82 ± 0.22	0.87 ± 0.17	0.30 ± 0.28
Tracts	0.73 ± 0.03	0.80 ± 0.04	0.65 ± 0.07	0.78 ± 0.08	0.65 ± 0.14
Connectome	0.69 ± 0.03	0.75 ± 0.05	0.61 ± 0.09	0.79 ± 0.11	0.51 ± 0.19
Tracts + HCV	0.73 ± 0.03	0.76 ± 0.05	0.69 ± 0.09	0.84 ± 0.10	0.54 ± 0.16
Connectome + HCV	0.71 ± 0.04	0.78 ± 0.06	0.63 ± 0.08	0.77 ± 0.11	0.62 ± 0.15

Table 4: Top 15 most important cortical connections for memory impairment classification ordered from most important (top) to less important (bottom). Cortical connections that preferentially had larger weights (i.e. impact on) for important PCs. lh = Left hemisphere; rh = Right hemisphere; ITG = Inferior temporal gyrus; MTG = Medial temporal gyrus

Cortical Connection
lh.temporalpole – lh.rostral-fusiform
rh.middle-ITG – rh.rostral-ITG
rh.caudal-fusiform – rh.rostral-ITG
lh.parahippocampal – lh.rostral-fusiform
rh.caudal-fusiform – rh.middle-fusiform
rh.caudal-MTG – rh.middle-precentral
lh.entorhinal – lh.isthmuscingulate
lh.caudal-MTG – lh.middle-precentral
lh.lingual – lh.caudal-fusiform
rh.caudal-ITG – rh.rostral-ITG
lh.temporalpole – lh.rostral-ITG
lh.inferiorparietal – lh.middle-ITG
lh.entorhinal – lh.precuneus
lh.inferiorparietal – lh.caudal-ITG
rh.parahippocampal – rh.middle-fusiform

REFERENCES

Alessio, A., Damasceno, B. P., Camargo, C. H., Kobayashi, E., Guerreiro, C. A., Cendes, F., 2004. Differences in memory performance and other clinical characteristics in patients with mesial temporal lobe epilepsy with and without hippocampal atrophy. Epilepsy and Behavior 5 (1), 22–27.

Alexander, A. L., Lee, J. E., Lazar, M., Field, A. S., 2007. Diffusion Tensor Imaging of the Brain. Neurotherapeutics 4 (3), 316–329.

Arbabshirani, M. R., Kiehl, K. A., Pearlson, G. D., Calhoun, V. D., 2013. Classification of schizophrenia patients based on resting-state functional network connectivity. Frontiers in Neuroscience 7 (7 JUL), 133.

Basser, P. J., Mattiello, J., Lebihan, D., 1994. Estimation of the Effective Self-Diffusion Tensor from the NMR Spin Echo. Journal of Magnetic Resonance, Series B 103 (3), 247–254.

Behrens, T. E., Berg, H. J., Jbabdi, S., Rushworth, M. F., Woolrich, M. W., 2007. Probabilistic diffusion tractography with multiple fibre orientations: What can we gain? NeuroImage 34 (1), 144–155.

Behrens, T. E., Woolrich, M. W., Jenkinson, M., Johansen-Berg, H., Nunes, R. G., Clare, S., Matthews, P. M., Brady, J. M., Smith, S. M., 2003. Characterization and propagation of uncertainty in diffusion-weighted MR imaging. Magnetic Resonance in Medicine 50 (5), 1077–1088.

Bernasconi, N., Bernasconi, A., Andermann, F., Dubeau, F., Feindel, W., Reutens, D. C., 1999. Entorhinal cortex in temporal lobe epilepsy: a quantitative MRI study. Neurology 52 (9), 1870.

Bernasconi, N., Bernasconi, A., Caramanos, Z., Antel, S. B., Andermann, F., Arnold, D. L., 2003. Mesial temporal damage in temporal lobe epilepsy: a volumetric MRI study of the hippocampus, amygdala and parahippocampal region. Brain 126 (2), 462–469.

Besson, P., Dinkelacker, V., Valabregue, R., Thivard, L., Leclerc, X., Baulac, M., Sammler, D., Colliot, O., Lehéricy, S., Samson, S., Dupont, S., 2014. Structural connectivity differences in left and right temporal lobe epilepsy. NeuroImage 100, 135–144.

Bonilha, L., Alessio, A., Rorden, C., Baylis, G., Damasceno, B. P., Min, L. L., Cendes, F., 2007. Extrahippocampal gray matter atrophy and memory impairment in patients with medial temporal lobe epilepsy. Human Brain Mapping 28 (12), 1376–1390.

Bonilha, L., Jensen, J. H., Baker, N., Breedlove, J., Nesland, T., Lin, J. J., Drane, D. L., Saindane, A. M., Binder, J. R., Kuzniecky, R. I., 2015. The brain connectome as a personalized biomarker of seizure outcomes after temporal lobectomy. Neurology 84 (18), 1846–53.

Brown, C. J., Hamarneh, G., 2016. Machine Learning on Human Connectome Data from MRI.

Budde, M. D., Janes, L., Gold, E., Turtzo, L. C., Frank, J. A., 2011. The contribution of gliosis to diffusion tensor anisotropy and tractography following traumatic brain injury: Validation in the rat using Fourier analysis of stained tissue sections. Brain 134 (8), 2248–2260.

Chen, J., Duan, X., Shu, H., Wang, Z., Long, Z., Liu, D., Liao, W., Shi, Y., Chen, H., Zhang, Z., 2016. Differential contributions of subregions of medial temporal lobe to memory system in amnestic mild cognitive impairment: Insights from fMRI study. Scientific Reports 6 (1), 26148.

Chen, T., Guestrin, C., 2016. XGBoost. In: Proceedings of the 22nd ACM SIGKDD International Conference on Knowledge Discovery and Data Mining. KDD '16. ACM, New York, NY, USA, pp. 785–794.

Cheng, W., Ji, X., Zhang, J., Feng, J., 2012. Individual classification of ADHD patients by integrating multiscale neuroimaging markers and advanced pattern recognition techniques. Frontiers in Systems Neuroscience 6, 58.

Craddock, R., Holtzheimer, P., Hu, X., Mayberg, H., 2009. Disease State Prediction from Resting State FMRI. NeuroImage 47 (6), S80.

Crossley, N. A., Mechelli, A., Scott, J., Carletti, F., Fox, P. T., Mcguire, P., Bullmore, E. T., 2014. The hubs of the human connectome are generally implicated in the anatomy of brain disorders. Brain 137 (8), 2382–2395.

Decarli, C., Hatta, J., Fazilat, S., Fazilat, S., Gaillard, W. D., Theodore, W. H., 1998. Extratemporal atrophy in patients with complex partial seizures of left temporal origin. Annals of neurology 43 (1), 41–45.

Delis, D., Kramer, J., Kaplan, E., BA, O., 2000. California Verbal Learning Test (California Verbal Learning Test-II). In: CVLT-II: California Verbal Learning Test: Adult Versionearning Test: Adult Version. Psychological Corporation, San Antonio.

Diehl, B., Busch, R. M., Duncan, J. S., Piao, Z., Tkach, J., Lüders, H. O., 2008. Abnormalities in diffusion tensor imaging of the uncinate fasciculus relate to reduced memory in temporal lobe epilepsy. Epilepsia 49 (8), 1409–1418.

Dodero, L., Quang, M. H., Biagio, M. S., Murino, V., Sona, D., 2015. KERNEL-BASED CLASSIFICATION FOR BRAIN CONNECTIVITY GRAPHS ON THE RIEMANNIAN MANIFOLD OF POSITIVE DEFINITE MATRICES Luca Dodero , H ' a Quang Minh , Marco San Biagio , Vittorio Murino and Diego Sona Pattern Analysis and Computer Vision , Istituto Italiano. In: 2015 IEEE 12th International Symposium on Biomedical Imaging (ISBI). IEEE, pp. 42–45.

Dreifuss, S., Vingerhoets, F. J. G., Lazeyras, F., Andino, S. G., Spinelli, L., Delavelle, J., Seeck, M., 2001. Volumetric measurements of subcortical nuclei in patients with temporal lobe epilepsy. Neurology 57 (9), 1636–1641.

Edmonds, E. C., Eppig, J., Bondi, M. W., Leyden, K. M., Goodwin, B., Delano-Wood, L., McDonald, C. R., Initiative, A. D. N., 2016. Heterogeneous cortical atrophy patterns in MCI not captured by conventional diagnostic criteria. Neurology 87 (20), 2108–2116.

Einstein, A., 1905. INVESTIGATIONS ON THE THEORY OF THE BROWNIAN MOVEMENT. Dover Publications Inc.

Engel, J., 2003. A Greater Role for Surgical Treatment of Epilepsy: Why and When? Epilepsy Currents 3 (2), 37–40.

Fisher, R. S., Vickrey, B. G., Gibson, P., Hermann, B., Penovich, P., Scherer, A., Walker, S., 2000. The impact of epilepsy from the patient's perspective I. Descriptions and subjective perceptions. Epilepsy Research 41 (1), 39–51.

Gastaut, H., Gastaut, J. L., Silva, G. E. e., Sanchez, G. R., 1975. Relative Frequency of Different Types of Epilepsy: A Study Employing the Classification of the International League Against Epilepsy. Epilepsia 16 (3), 457–461.

Gleichgerrcht, E., Munsell, B., Bhatia, S., Vandergrift, W. A., Rorden, C., McDonald, C., Edwards, J., Kuzniecky, R., Bonilha, L., 2018. Deep learning applied to whole-brain connectome to determine seizure control after epilepsy surgery. Epilepsia 59 (9), 1643–1654.

Griffith, H. R., Pyzalski, R. W., O'Leary, D., Magnotta, V., Bell, B., Dow, C., Hermann, B., Seidenberg, M., 2003. A Controlled Quantitative MRI Volumetric Investigation

of Hippocampal Contributions to Immediate and Delayed Memory Performance. Journal of Clinical and Experimental Neuropsychology 25 (8), 1117–1127.

Griffith, H. R., Pyzalski, R. W., Seidenberg, M., Hermann, B. P., 2004. Memory relationships between MRI volumes and resting PET metabolism of medial temporal lobe structures. Epilepsy and Behavior 5 (5), 669–676.

Hagler, D. J., Ahmadi, M. E., Kuperman, J., Holland, D., McDonald, C. R., Halgren, E., Dale, A. M., Halgren, E., Holland, D., Kuperman, J., Hagler, D. J., 2009. Automated white-matter tractography using a probabilistic diffusion tensor atlas: Application to temporal lobe epilepsy. Human Brain Mapping 30 (5), 1535–1547.

Hagmann, P., Kurant, M., Gigandet, X., Thiran, P., Wedeen, V. J., Meuli, R., Thiran, J.-P., 2007. Mapping Human Whole-Brain Structural Networks with Diffusion MRI. PLoS ONE 2 (7), e597.

Helmstaedter, C., Grunwald, T., Lehnertz, K., Gleissner, U., E., E. C., 1997. Differential involvement of left temporolateral and temporomesial structures in verbal declarative learning and memory: Evidence from temporal lobe epilepsy. Brain and Cognition 35 (1), 110–131.

Helmstaedter, C., Kurthen, M., Lux, S., Reuber, M., Elger, C. E., 2003. Chronic epilepsy and cognition: A longitudinal study in temporal lobe epilepsy. Annals of Neurology 54 (4), 425–432.

Hermann, B., Seidenberg, M., Bell, B., Rutecki, P., Sheth, R. D., Wendt, G., O'Leary, D., Magnotta, V., 2003. Extratemporal quantitative MR volumetrics and neuropsychological status in temporal lobe epilepsy.

Hermann, B. P., Bayless, K., Hansen, R., Parrish, J., Seidenberg, M., 2005. Cerebellar atrophy in temporal lobe epilepsy. Epilepsy & Behavior 7 (2), 279–287.

Hermann, B. P., Seidenberg, M., 2008. Behavioral Aspects of Epilepsy: Principles and Practice. Demos Medical Publishing, New York.

Hermann, B. P., Seidenberg, M., Dow, C., Jones, J., Rutecki, P., Bhattacharya, A., Bell, B., 2006. Cognitive prognosis in chronic temporal lobe epilepsy. Annals of Neurology 60 (1), 80–87.

Hermann, B. P., Wyler, A. R., Somes, G., Berry, A. D., Dohan, F. C., 1992. Pathological Status of the Mesial Temporal Lobe Predicts Memory Outcome from Left Anterior Temporal Lobectomy. Neurosurgery 31 (4), 652–657.

Hernández, M., Guerrero, G. D., Cecilia, J. M., García, J. M., Inuggi, A., 2013. Accelerating Fibre Orientation Estimation from Diffusion Weighted Magnetic Resonance Imaging Using GPUs. PLoS ONE 8 (4), 61892.

Hernandez-Fernandez, M., Reguly, I., Giles, M., Jbabdi, S., Smith, S., Sotiropoulos, S. N., 2016. A fast and flexible toolbox for tracking brain connections in diffusion MRI datasets using GPUs. In: 22nd Annual Meeting of the Organization for Human Brain Mapping (OHBM). Geneva, Switzerland.

Hirni, D. I., Kivisaari, S. L., Monsch, A. U., Taylor, K. I., 2013. Distinct neuroanatomical bases of episodic and semantic memory performance in Alzheimer's disease. Neuropsychologia 51 (5), 930–937.

Holland, D., Kuperman, J. M., Dale, A. M., 2010. Efficient correction of inhomogeneous static magnetic field-induced distortion in Echo Planar Imaging. NeuroImage 50 (1), 175–183.

Kalilani, L., Sun, X., Pelgrims, B., Noack-Rink, M., Villanueva, V., 2018. The epidemiology of drug-resistant epilepsy: A systematic review and meta-analysis. Epilepsia 59 (12), 2179–2193.

Kilpatrick, C., Murrie, V., Cook, M., Andrewes, D., Desmond, P., Hopper, J., 1997. SEVERITY OF VERBAL MEMORY DEFICITS CORRELATES WITH DEGREE OF LEFT HIPPOCAMPAL ATROPHY. Epilepsia 6 (3), 213–218.

Kuzniecky, R., Bilir, E., Gilliam, F., Faught, E., Martin, R., Hugg, J., 1999. Quantitative MRI in temporal lobe epilepsy: evidence for fornix atrophy. Neurology 53 (3), 496.

Le Bihan, D., 1991. Molecular diffusion nuclear magnetic resonance imaging. Magnetic resonance quarterly 7 (1), 1–30.

Le Bihan, D., Mangin, J. F., Poupon, C., Clark, C. A., Pappata, S., Molko, N., Chabriat, H., 2001. Diffusion tensor imaging: Concepts and applications. Journal of Magnetic Resonance Imaging 13 (4), 534–546.

Lencz, T., McCarthy, G., Bronen, R. A., Scott, T. M., Inserni, J. A., Sass, K. J., Novelly, R. A., Kim, J. H., Spencer, D. D., 1992. Quantitative magnetic resonance imaging in temporal lobe epilepsy: relationship to neuropathology and neuropsychological function. Annals of Neurology: Official Journal of the American Neurological Association and the Child Neurology Society 31 (6), 629–637.

Lin, C. P., Tseng, W. Y. I., Cheng, H. C., Chen, J. H., 2001. Validation of diffusion tensor magnetic resonance axonal fiber imaging with registered manganese-enhanced optic tracts. NeuroImage 14 (5), 1035–1047.

Lui, Y. W., Nusbaum, A. O., Barr, W. B., Johnson, G., Babb, J. S., Orbach, D., Kim, A., Laliotis, G., Devinsky, O., 2005. Correlation of apparent diffusion coefficient with neuropsychological testing in temporal lobe epilepsy. American Journal of Neuroradiology 26 (7), 1832–1839.

McDonald, C. R., 2008. The use of neuroimaging to study behavior in patients with epilepsy. Epilepsy and Behavior 12 (4), 600–611.

McDonald, C. R., Ahmadi, M. E., Hagler, D. J., Tecoma, E. S., Iragui, V. J., Gharapetian, L., Dale, A. M., Halgren, E., 2008. Diffusion tensor imaging correlates of memory and language impairments in temporal lobe epilepsy. Neurology 71 (23), 1869–1876.

McDonald, C. R., Leyden, K. M., Hagler, D. J., Kucukboyaci, N. E., Kemmotsu, N., Tecoma, E. S., Iragui, V. J., 2014. White matter microstructure complements morphometry for predicting verbal memory in epilepsy. Cortex 58, 139–150.

Milner, B., 1970. MEMORY AND THE MEDIAL TEMPORAL REGIONS OF THE BRAIN. In: Pribram, K. H., Broadbent, D. E. (Eds.), Biology of Memory. Academic Press, New York, Ch. 6, pp. 29–50.

Moyer, D., Gutman, B., Prasad, G., Faskowitz, J., Ver Steeg, G., Thompson, P., 2015. Blockmodels for connectome analysis. In: 11th International Symposium on Medical Information Processing and Analysis. Vol. 9681. International Society for Optics and Photonics, p. 96810A.

Natsume, J., Bernasconi, N., Andermann, F., Bernasconi, A., 2003. MRI volumetry of the thalamus in temporal, extratemporal, and idiopathic generalized epilepsy. Neurology 60 (8), 1296–1300.

Ngugi, A. K., Bottomley, C., Kleinschmidt, I., Sander, J. W., Newton, C. R., 2010. Estimation of the burden of active and life-time epilepsy: A meta-analytic approach. Epilepsia 51 (5), 883–890.

Pierpaoli, C., Basser, P. J., 1996. Toward a quantitative assessment of diffusion anisotropy. Magnetic Resonance in Medicine 37 (6), 972.

Reyes, A., Kaestner, E., Bahrami, N., Balachandra, A., Hegde, M., Paul, B. M., Hermann, B., McDonald, C. R., 2019. Cognitive phenotypes in temporal lobe epilepsy are associated with distinct patterns of white matter network abnormalities. Neurology 92 (17), e1957–e1968.

Riley, J. D., Franklin, D. L., Choi, V., Kim, R. C., Binder, D. K., Cramer, S. C., Lin, J. J., 2010. Altered white matter integrity in temporal lobe epilepsy: Association with cognitive and clinical profiles. Epilepsia 51 (4), 536–545.

Rosa, M. J., Portugal, L., Shawe-Taylor, J., Mourao-Miranda, J., 2013. Sparse Network-Based Models for Patient Classification Using fMRI. 2013 International Workshop on Pattern Recognition in Neuroimaging 105, 66–69.

Rosenberg, M. D., Finn, E. S., Scheinost, D., Papademetris, X., Shen, X., Constable, R. T., Chun, M. M., 2015. A neuromarker of sustained attention from whole-brain functional connectivity. Nature Neuroscience 19 (1), 165–171.

Sacchet, M. D., Prasad, G., Foland-ross, L. C., Thompson, P. M., Gotlib, I. H., 2015. Support vector machine classification of Major Depressive Disorder using diffusion-weighted neuroimaging and graph theory. Frontiers in psychiatry 6, 21.

Saling, M. M., 2009. Verbal memory in mesial temporal lobe epilepsy: Beyond material specificity. Brain 132 (3), 570–582.

Salmenperä, T., Kälviäinen, R., Partanen, K., Pitkänen, A., 2001. Hippocampal and amygdaloid damage in partial epilepsy: a cross-sectional MRI study of 241 patients. Epilepsy research 46 (1), 69–82.

Sandok, E. K., O'brien, T. J., Jack, C. R., So, E. L., 2000. Significance of cerebellar atrophy in intractable temporal lobe epilepsy: a quantitative MRI study. Epilepsia 41 (10), 1315–1320.

Shallice, T., Fletcher, P., Frith, C. D., Grasby, P., Frackowiak, R. S., Dolan, R. J., 1994. Brain regions associated with acquisition and retrieval of verbal episodic memory. Nature 368 (6472), 633–635.

Shen, H., Wang, L., Liu, Y., Hu, D., 2010. Discriminative analysis of resting-state functional connectivity patterns of schizophrenia using low dimensional embedding of fMRI. NeuroImage 49 (4), 3110–3121.

Slinger, G., Sinke, M. R., Braun, K. P., Otte, W. M., 2016. White matter abnormalities at a regional and voxel level in focal and generalized epilepsy: A systematic review and meta-analysis. NeuroImage: Clinical 12, 902–909.

Smith, S. M., 2002. Fast robust automated brain extraction. Human brain mapping 17 (3), 143–55.

Sporns, O., Tononi, G., Kötter, R., 2005. The human connectome: A structural description of the human brain. PLoS Computational Biology 1 (4), 0245–0251.

Szabo, C. A., Lancaster, J. L., Lee, S., Xiong, J.-H., Cook, C., Mayes, B. N., Fox, P. T., 2006. MR imaging volumetry of subcortical structures and cerebellar hemispheres in temporal lobe epilepsy. American Journal of Neuroradiology 27 (10), 2155–2160.

Taylor, P. N., Sinha, N., Wang, Y., Vos, S. B., de Tisi, J., Miserocchi, A., McEvoy, A. W., Winston, G. P., Duncan, J. S., 2018a. The impact of epilepsy surgery on the structural connectome and its relation to outcome. NeuroImage: Clinical 18 (December 2017), 202–214.

Taylor, P. N., Sinha, N., Wang, Y., Vos, S. B., de Tisi, J., Miserocchi, A., McEvoy, A. W., Winston, G. P., Duncan, J. S., 2018b. The impact of epilepsy surgery on the structural connectome and its relation to outcome. NeuroImage: Clinical 18 (January), 202–214.

Téllez-Zenteno, J. F., Dhar, R., Wiebe, S., 2005. Long-term seizure outcomes following epilepsy surgery: A systematic review and meta-analysis. Brain 128 (5), 1188–1198.

Voets, N. L., Zamboni, G., Stokes, M. G., Carpenter, K., Stacey, R., Adcock, J. E., 2014. Aberrant Functional Connectivity in Dissociable Hippocampal Networks Is Associated with Deficits in Memory. Journal of Neuroscience 34 (14), 4920–4928.

Wakana, S., Caprihan, A., Panzenboeck, M. M., Fallon, J. H., Perry, M., Gollub, R. L., Hua, K., Zhang, J., Jiang, H., Dubey, P., Blitz, A., van Zijl, P., Mori, S., 2007. Reproducibility of quantitative tractography methods applied to cerebral white matter. NeuroImage 36 (3), 630–644.

Warach, S., Chien, D., Li, W., Ronthal, M., Edelman, R. R., 1992. Fast magnetic resonance diffusion-weighted imaging of acute human stroke. Neurology 42 (9), 1717–1717.

Wechsler, D., 1997. WMS-III: Wechsler Memory Scale Administration and Scoring Manual.

Wieser, H., 2004. Mesial temporal lobe epilepsy with hippocampal sclerosis. Epilepsia 45 (6), 695–714.

Wong, M., Guo, D., 2013. Dendritic spine pathology in epilepsy: Cause or consequence?